2900-394-T

Report of Project MICHIGAN

SIGNAL DETECTION BY COMPLEX SPATIAL FILTERING

A. B. VANDER LUGT

July 1963

Radar Laboratory
Institute of Science and Technology
THE UNIVERSITY OF MICHIGAN
Ann Arbor, Michigan

NOTICES

Sponsorship. The work reported herein was conducted by the Institute of Science and Technology for the U. S. Army Electronics Command under Project MICHIGAN. Contract DA-36-039 SC-78801, and for the U. S. Air Force under Contract AF 33(616)-8433. Contracts and grants to The University of Michigan for the support of sponsored research by the Institute of Science and Technology are administered through the Office of the Vice-President for Research.

Note. The views expressed herein are those of Project MICHIGAN and have not been approved by the Department of the Army.

Distribution. Initial distribution is indicated at the end of this document. Distribution control of Project MICHIGAN documents has been delegated by the U. S. Army Electronics Command to the office named below. Please address correspondence concerning distribution of reports to:

Commanding Officer
U. S. Army Liaison Group
Project MICHIGAN
The University of Michigan
P. O. Box 618
Ann Arbor, Michigan

ASTIA Availability. Qualified requesters may obtain copies of this document from:

Armed Services Technical Information Agency
Arlington Hall Station
Arlington 12, Virginia

Final Disposition. After this document has served its purpose, it may be destroyed. Please do not return it to the Institute of Science and Technology.

PREFACE

Project MICHIGAN is a continuing, long-range research and development program for advancing the Army's combat-surveillance and target-acquisition capabilities. The program is carried out by a full-time Institute of Science and Technology staff of specialists in the fields of physics, engineering, mathematics, and psychology, by members of the teaching faculty, by graduate students, and by other research groups and laboratories of The University of Michigan.

The emphasis of the Project is upon research in imaging radar, MTI radar, infrared, radio location, image processing, and special investigations. Particular attention is given to all-weather, long-range, high-resolution sensory and location techniques.

Project MICHIGAN was established by the U. S. Army Signal Corps at The University of Michigan in 1953 and has received continuing support from the U. S. Army. The Project constitutes a major portion of the diversified program of research conducted by the Institute of Science and Technology in order to make available to government and industry the resources of The University of Michigan and to broaden the educational opportunities for students in the scientific and engineering disciplines.

Progress and results described in reports are continually reassessed by Project MICHIGAN. Comments and suggestions from readers are invited.

Robert L. Hess
Director
Project MICHIGAN

CONTENTS

FIGURES

GLOSSARY

A	amplitude of illumination; system half-aperture
k, k', a, b, c	constants
d	distance
D	density
E	exposure; expected value
f	function representing the available data; focal length of lens
g	function representing the scene
G	filter function
h	impulse response of filter
I	indicator function
k	$2\pi/\lambda$
m	scaling factor
n	noise; refractive index
p, q	spatial radian frequencies
r	output of processing system; distance
R	reference wave; correlation function
s	signal
T	transformation; transmission; thickness
x, y, ξ, η, u, v	space coordinates
X	range on signal for space-invariant operation
ϵ	error term
ψ	lens aberrations
ϕ, θ	phase portion of complex functions; angles
λ	wavelength of light
γ	gamma of film

SIGNAL DETECTION BY COMPLEX SPATIAL FILTERING

ABSTRACT

This report contains integrated descriptions of the problem of signal detection, the optimum linear filtering process, a coherent optical system which accomplishes this filtering process, and a technique for realizing the required complex filter. Experimental results show that the theory is valid.

The appendixes give a treatment of the Fourier transforming property of lenses which is general enough that complete optical systems can be evaluated on the basis of frequency response and region of space-invariant operation.

The experimental results obtained to date indicate that this technique provides an excellent two-dimensional filtering capability that will play a key role in problems such as shape recognition and signal detection.

1
INTRODUCTION

The fundamental theory of optical spatial filtering has been formulated by several writers [1-3]. The close analogy of spatial filtering to optimum linear filtering theory promised to open up new techniques for realizing those frequency domain filters which could not be synthesized in the time domain because of the realizability contraint. But the advances in spatial filtering since the formulation of the theory have not been what one might have expected. Perhaps the major reason is that, whereas the theoretical formulation tacitly assumed that complex filters could be realized, the actual realization has presented a difficult problem. It was generally assumed that photographic transparencies would play a large role in the realization of spatial filters [2, 3], but any hope for making complex filters on film has seemed remote. Some work was aimed in this direction [4, 5], but it is not directly applicable to the problem treated in this report.

Since spatial filters are passive, they can take on all values on or within the unit circle in the complex plane [6]. Early experiments in spatial filtering used occluding filters as bandpass filters to demonstrate the theory. Later, continuous amplitude control, such as Gaussian weighting, was used to show how equalization could be accomplished by optical systems. The next step was to add binary phase control to extend the range of filter values to the entire real line. Binary control was gained by using ruled phase plates, evaporation techniques, or film reliefing techniques. Not only are these techniques awkward to apply, but, more seriously, the impulse response of a real filter is symmetrical. Clearly, if more general filtering schemes are to be performed, a fairly easy method of constructing the general complex filter must be found. This report describes, as one of its major results, a practical technique for realizing a general complex filter even though the filter function is recorded on photographic film.

In most other approaches to the problem of the realization of the desired complex filter, a complex distribution of light must be analyzed. This report shows how, at the same time, the analysis can be avoided and the complex filter can be realized. This feature is important since the required filter can be found analytically for only a few simple two-dimensional functions.

This report contains an integrated description of the problem of signal detection, the optimum filtering process, a coherent optical system which accomplishes this filtering process, and a technique for realizing the required complex filter. The appendixes give some important insight into the Fourier transforming properties of a lens system operating under coherent illumination. The theory, which is more general than usual, is used to discuss and evaluate several optical systems.

2
MATHEMATICAL NATURE OF THE PROBLEM

The mathematical model shown in Figure 1 describes the problem of sensing, recording, and processing imagery. The scene will be denoted by g(x, y), an intensity function of two space coordinates. The sensor makes a two-dimensional transformation of g(x, y), and the recording process transforms it further. Because the recording medium is usually photographic film, film grain becomes a secondary source of noise. The processing of the imagery is equivalent to a third transformation on g(x, y), and the output is an estimation of the amount of signal present in g(x, y).

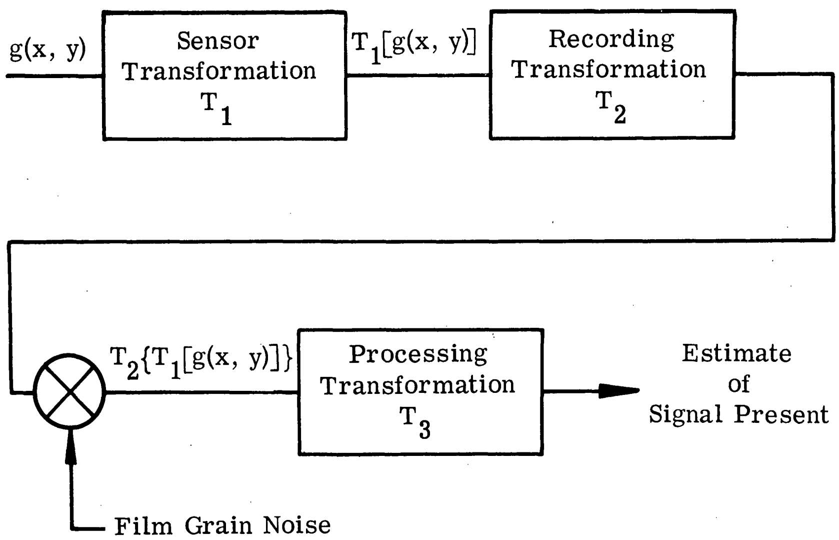

FIGURE 1. MATHEMATICAL MODEL FOR IMAGE PROCESSING

It has become common practice to refer to

$$f(x, y) = T_2\{T_1[g(x, y)]\}$$

as the "scene." Although this is not strictly correct, transformation T_2 is usually a nonlinear process, and a poorly controlled one at that; therefore, it becomes necessary to operate on the available data f(x, y) rather than to attempt to recover g(x, y) before the processing operation.

3
OPTIMUM FILTERING

Suppose n(x, y) is a homogeneous isotropic random process with spectral density N(p, q), and s(x, y) is a known Fourier transformable function of space coordinates. We wish to operate on f(x, y) = s(x, y) + n(x, y) in such a way that we maximize the ratio of peak signal energy to mean square noise energy in the output. Suppose h(x, y) is the impulse response of a linear, space invariant filter with frequency response H(p, q). It is desirable to determine an optimum filter under the condition stated. See Figure 2.

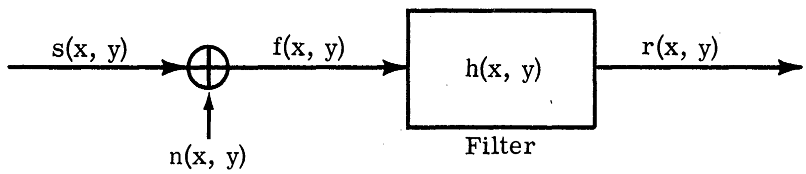

FIGURE 2. PROCESSING SYSTEM

The signal part of the output is

$$r_s(x, y) = \frac{1}{4\pi^2} \iint_{-\infty}^{\infty} S(p, q)\, H(p, q)\, e^{j(px+qy)}\, dp\, dq$$

and

$$\text{MSN (mean square noise)} = \frac{1}{4\pi^2} \iint_{-\infty}^{\infty} N(p, q)\, |H(p, q)|^2\, dp\, dq$$

We want to find maximum over all $\{H(p, q)\}$ for the ratio $\frac{|r_s(0, 0)|^2}{\text{MSN}}$, where the peak signal is taken at (0, 0) for convenience. We have

$$\frac{|r_s(0,\ 0)|^2}{\text{MSN}} = \frac{\left|\frac{1}{4\pi^2}\iint\limits_{-\infty}^{\infty} S(p,\ q)\ H(p,\ q)\, dp\, dq\right|^2}{\frac{1}{4\pi^2}\iint\limits_{-\infty}^{\infty} N(p,\ q)\ |H(p,\ q)|^2\, dp\, dq} \tag{1}$$

For nontrivial cases, $N(p, q) > 0$ for all (p, q), so that it can be treated as the weighting function in the Schwarz inequality. Rewrite Equation 1 in the form

$$\frac{|r_s(0,\ 0)|^2}{\text{MSN}} = \frac{\frac{1}{4\pi^2}\left|\iint\limits_{-\infty}^{\infty} \left[\frac{S(p,\ q)}{N(p,\ q)}\right] H(p,\ q)\ N(p,\ q)\, dp\, dq\right|^2}{\iint\limits_{-\infty}^{\infty} |H(p,\ q)|^2\ N(p,\ q)\, dp\, dq} \tag{2}$$

Apply the Schwarz inequality to the numerator of Equation 2 to get

$$\underset{\{H\}}{\text{Max}}\ \frac{|r_s(0,\ 0)|^2}{\text{MSN}} \le \frac{\frac{1}{4\pi^2}\left[\iint\limits_{-\infty}^{\infty} \left|\frac{S(p,\ q)}{N(p,\ q)}\right|^2 N(p,\ q)\, dp\, dq\right]\left[\iint\limits_{-\infty}^{\infty} |H(p,\ q)|^2\, N(p,\ q)\, dp\, dq\right]}{\iint\limits_{-\infty}^{\infty} |H(p,\ q)|^2\ N(p,\ q)\, dp\, dq}$$

$$\le \frac{1}{4\pi^2}\iint\limits_{-\infty}^{\infty} \left|\frac{S(p,\ q)}{N(p,\ q)}\right|^2 N(p,\ q)\, dp\, dq$$

We get a maximum on H when

$$H(p,\ q) = k\,\frac{\overline{S(p,\ q)}}{N(p,\ q)} \tag{3}$$

(where the bar indicates a complex conjugate) and the signal-to-noise ratio is

$$S/N = \frac{1}{4\pi^2}\iint\limits_{-\infty}^{\infty} \frac{|S(p,\ q)|^2}{N(p,\ q)}\, dp\, dq \tag{4}$$

From Equation 3 we see that under the given constraints the optimum filter is proportional to the complex conjugate of the signal spectrum divided by the noise spectral density. The output of the system is given by

$$r(x, y) = \frac{1}{4\pi^2} \iint_{-\infty}^{\infty} F(p, q)\, H(p, q)\, e^{j(px+qy)}\, dp\, dq \qquad (5)$$

In case N(p, q) is uniform for all frequencies we have

$$H(p, q) = k' \overline{S(p, q)}$$

and

$$r(x, y) = \frac{k'}{4\pi^2} \iint_{-\infty}^{\infty} F(p, q)\, \overline{S(p, q)}\, e^{j(px+qy)}\, dp\, dq$$

Employing the convolution theorem, we have

$$r(x, y) = k' \iint_{-\infty}^{\infty} f(x_o, y_o)\, \overline{s(-x + x_o, -y + y_o)}\, dx_o\, dy_o$$

$$= k' \iint_{-\infty}^{\infty} f(x + u, y + v)\, \overline{s(u, v)}\, du\, dv \qquad (6)$$

which is a cross-correlation process. Optical systems which perform the operations indicated by Equations 5 and 6 will be described in Section 4.

An interesting situation arises when the signal and noise are not linearly additive, but are mutually exclusive processes. Then the signal is no longer a known function, but becomes a random process. This case arises when the signal is partially occluded by noise, and also when film grain noise is present. The mutually exclusive noise situation is analyzed in Appendix A.

4
OPTICAL PROCESSING SYSTEMS

4.1. COHERENT OPTICAL SYSTEMS

Optimum filter theory makes widespread use of Fourier transform theory to arrive at results easily. Unfortunately, since the synthesis of an electronic filter must be made in the time domain, there are restrictions on the realizability of the filter, as well as some limitations on its performance. The use of a coherent optical system overcomes some of these restrictions because it can display the Fourier analysis of signals as a distribution of light, and one has the option of constructing the filter in either the frequency or the space domain.

The optical system shown in Figure 3 acts as a two-dimensional Fourier analyzer, as is shown in Appendix B. If f(x, y) denotes the specular amplitude transmission of the transparency in plane P_1 and F(p, q) denotes the complex amplitude distribution of light in plane P_2, then

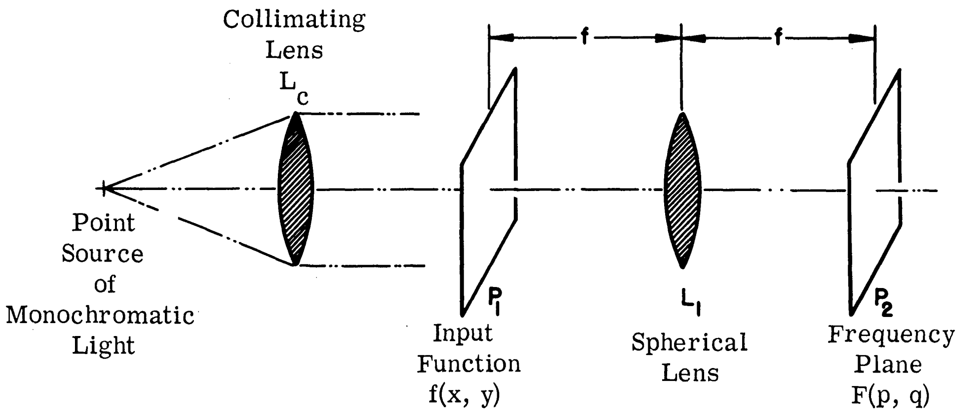

FIGURE 3. AN OPTICAL FOURIER ANALYZER

$$F(p, q) = \iint_{-\infty}^{\infty} f(x, y)\, e^{j(px+qy)}\, dx\, dy \tag{7}$$

when d = f and the illumination is a monochromatic plane wave. In Equation 7 p and q represent spatial frequency variables having the dimensions of radians/unit distance. But the variables in plane P_2 are in units of distance which are

$$\xi = \frac{\lambda f p}{2\pi}$$

$$\eta = \frac{\lambda f q}{2\pi}$$

where ξ = the direction parallel to x

η = the direction parallel to y

λ = the wavelength of the illumination

f = the focal length of the spherical lens

In general, the variables (p, q) will be used for emphasis when a distribution of light is a function of frequency, as well as to simplify the notation associated with Fourier transform theory.

A transform relationship can exist under a wide variety of conditions. If $d \neq f$, then $F(\xi, \eta)$ is modified by a quadratic phase factor which does not affect the intensity of the distribution. Also, convergent or divergent illumination will only relocate plane P_2, which changes the scale of $F(\xi, \eta)$ as well as modifying $F(\xi, \eta)$ by a spherical phase factor. These phase terms serve only to determine the position of the image plane for the input transparency, or else the position of the frequency plane (plane P_2). These conditions are discussed in Appendix B in connection with the frequency response of optical systems.

The fact that a spherical lens can take the Fourier transform of a complex distribution of light allows one to construct an optical system by arranging a sequence of lenses which forms a succession of Fourier transform planes. An image of the input plane can be effected by placing a lens behind plane P_2 which takes the transform of F(p, q) (see Figure 4). Since a positive

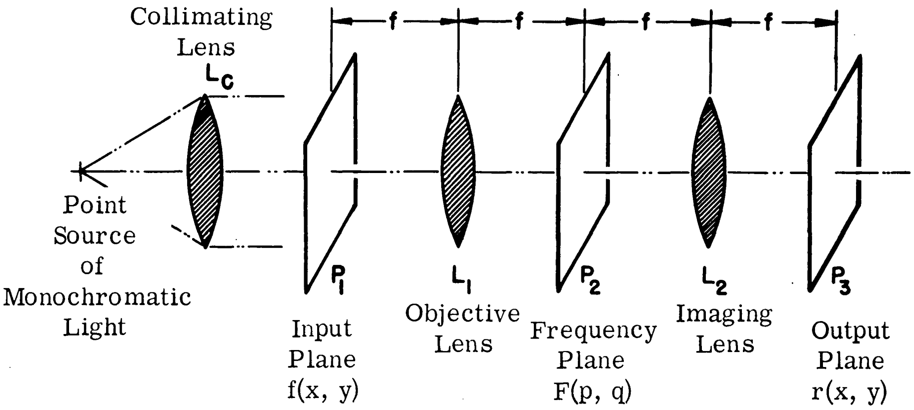

FIGURE 4. A COHERENT PROCESSING SYSTEM

spherical lens always introduces a positive kernel in the transform relationship, we have in plane P_3 the distribution

$$r(x, y) = \frac{1}{4\pi^2} \iint_{-\infty}^{\infty} F(p, q)\, e^{j(px+qy)}\, dp\, dq$$

$$= f(-x, -y)$$

We have assumed that the system has unity magnification and sufficient bandwidth to pass the highest spatial frequency in the input function. Note that the output is an inverted image of the input function, which is what one expects from an imaging system operating under any type of illumination. We have also assumed that the lenses have no aberrations and that the system is space-invariant. Limitations placed on the system to assure space invariance for a given bandwidth signal are discussed in Appendix B.

In certain conditions the optical system in Figure 4 can be made to operate as a cross-correlator. Suppose a transparency is placed in plane P_2, whose transmission is given by H(p, q). The modified light distribution in this plane is now

$$R(p, q) = F(p, q)\, H(p, q)$$

Lens L_2 takes the Fourier transform of this distribution and displays it in plane P_3 as

$$r(x, y) = \frac{1}{4\pi^2} \iint_{-\infty}^{\infty} F(p, q)\, H(p, q)\, e^{j(px+qy)}\, dp\, dq$$

By use of the convolution theorem,

$$r(x, y) = \iint_{-\infty}^{\infty} f(x - u, y - v)\, h(u, v)\, du\, dv$$

If N(p, q) is uniform for all (p, q) of interest, the optimum filter is $H(p, q) = k_1 \overline{S(p, q)}$, and

$$r(x, y) = k_1 f(x, y) * \overline{s(x, y)}$$

which is the cross-correlation of the signal with the input transparency (* denotes convolution).

If two transparencies are placed in contact, their complex transmissions are multiplicative.[1] Consequently, to synthesize the filter described in Equation 3, we need to insert a transparency whose transmission is 1/N(p, q) in plane P_2 in addition to the transparency representing $\overline{S(p, q)}$. When this filter is used, the output of the system essentially represents the probability that a signal has occurred at any point in the input; a bright spot in the output indicates high probability, whereas low light levels indicate low probability. This process simultaneously detects all signals with similar orientations in any location in P_1, as can be seen by observing that the spectrum of a translated signal is modified by a linear phase factor. This phase factor contains precisely the information required to image the signal at the proper position in the output. In contrast, the system is sensitive to the orientation of the signal; but a rotation of the filter relative to the input will detect these signals sequentially.

Other optical configurations will perform the required operation, but the configuration shown in Figure 4 is most convenient and has optimum frequency response. The process could be carried out with two lenses or even a single lens. These configurations are discussed in Appendix B.

4.2. NONCOHERENT OPTICAL SYSTEMS

Noncoherent optical systems have limited usefulness, since they can be used only when N(p, q) = N for all (p, q) of interest. This restriction frequently results in processing such a small amount of data that the system becomes impractical. The noncoherent system is further

[1] Unless otherwise noted, the word "transmission" will be used in this report to refer to specular amplitude transmission of the transparency.

limited by the fact that f(x, y) must be real. Since a noncoherent system does not exhibit a frequency plane similar to that of a coherent system, H(p, q) must be realized in the space domain. The problem is to design a system with impulse response

$$h(x, y) = \frac{k'}{4\pi} \iint_{-\infty}^{\infty} \overline{S(p, q)}\, e^{j(px+qy)}\, dp\, dq$$

$$= k_1\, \overline{s(-x, -y)}$$

This result can be accomplished easily by using a reference function optical system. In the optical system shown in Figure 5, plane P_1 is an extended source of diffuse illumination (not necessarily monochromatic). The transparency representing f(x, y) is placed in plane P_2, and the reference function representing h(x, y) is placed in plane P_3. Since the signal is real, h(x, y) = s(-x, -y). A ray of light from a point (x_1, y_1) in plane P_1 passes through the point (x_2, y_2) in plane P_2 and is attenuated by $f(x_2, y_2)$. This ray passes through the reference

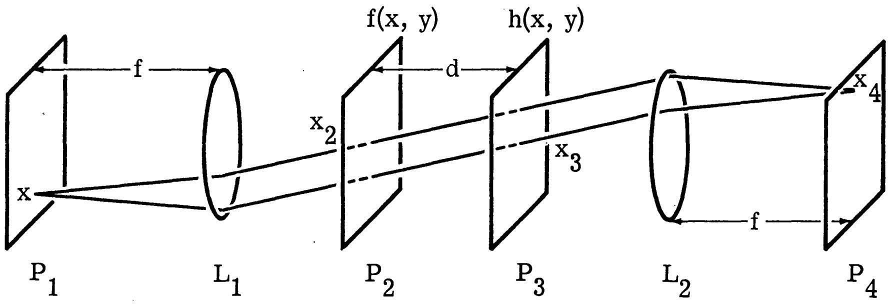

FIGURE 5. A NONCOHERENT PROCESSING SYSTEM

function at a point (x_3, y_3) and is further attenuated by a factor $s(-x_3, -y_3)$. From the geometry we see that

$$\frac{x_4}{f} = \frac{x_2 - x_3}{d}$$

$$\frac{y_4}{f} = \frac{y_2 - y_3}{d}$$

The intensity of light in the image of the point (x_1, y_1) is the summation of all rays parallel to the ray described; i.e.,

$$r(x_4, y_4) = \iint_{-\infty}^{\infty} f(x_2, y_2)\, s(-x_3, -y_3)\, dx_3\, dy_3$$

$$= \iint_{-\infty}^{\infty} f(x_2, y_2)\, s\left(\frac{x_4 d}{f} - x_2, \frac{y_4 d}{f} - y_2\right) dx_2\, dy_2$$

By a change of variables we have

$$r(x, y) = k \iint_{-\infty}^{\infty} f(x + u, y + v)\, s(u, v)\, du\, dv$$

which is the desired output. The constraint on N(p, q) limits the usefulness of the noncoherent system.

5
REALIZATION OF THE OPTIMUM FILTER

Having determined that the optimum filter which maximizes the ratio of peak signal energy to mean square noise energy is given by Equation 3, we must find some method to realize H(p, q). Except for the fact that H(p, q) is usually a complex quantity, photographic film would be the prime candidate for recording the filter. But only when H(p, q) is nonnegative can it be realized on film.

Since N(p, q) > 0 for the nontrivial case, it can always be realized on film. Recall that N(p, q) can be found by averaging over an ensemble of sample functions. A better approximation to N(p, q) can usually be found by dividing sample functions into subclasses with distinctly different noise structures. (A class might be all backgrounds consisting of natural terrain, or the structure associated with populated areas, or the background structure associated with radar returns, etc.) Since a priori knowledge exists as to which class of noise functions is being processed, the appropriate N(p, q) can be selected.

5.1. REALIZATION OF NONNEGATIVE FILTERS

The first step in realizing any function on photographic film is a brief review of the film's transfer characteristics. A typical curve of density versus long exposure is shown in Figure 6. This curve is characterized in its linear region by

$$D_n = \gamma_n (\log E_n - \log E_o) \tag{8}$$

where γ_n is the slope of the straight line
E_n is the exposure
E_o is the intercept of the straight line
D_n is the intensity density
n means that a negative transparency is used

The coherent system operates on the transmission of the film so that

$$T = e^{-D/2} \tag{9}$$

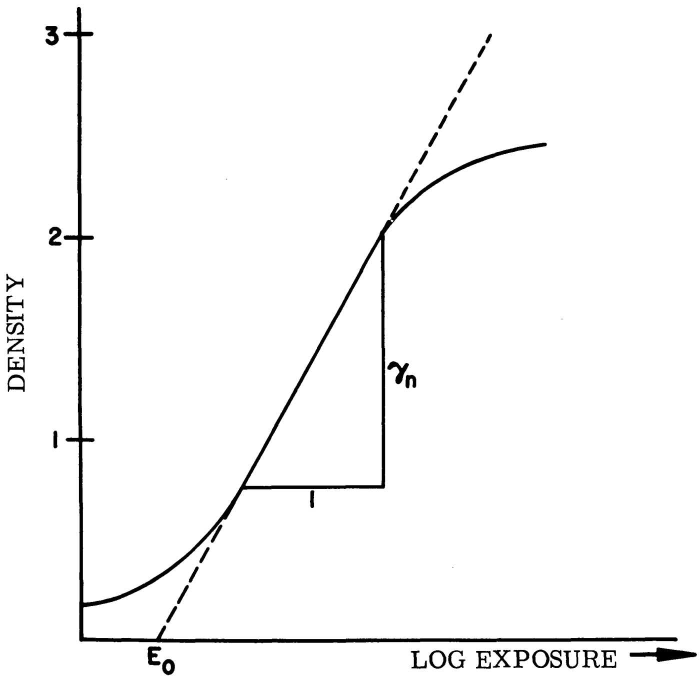

FIGURE 6. TYPICAL CURVE OF DENSITY VS. LOG EXPOSURE

or

$$T_n = \frac{C}{E_n^{\gamma_n/2}} \tag{10}$$

If we make E_n proportional to N(p, q) and require $\gamma_n = 2$, we have realized the denominator of H(p, q). The exposure can be made proportional to N(p, q) by photographing a rotating sector of a circle. Since n(x, y) is assumed to be isotropic, N(p, q) is rotationally symmetric. The sector is constructed so that

$$\frac{s(\rho)}{2\pi\rho} \propto N(\rho) \qquad \rho = \sqrt{p^2 + q^2} \tag{11}$$

where $s(\rho)$ is the arc length at radius ρ; see Figure 7. This sector, uniformly illuminated, is rotated many times during the exposure interval, with the result that $E \propto N(\rho)$ and $T_n = C/N(\rho)$. This process must be modified in order to realize the numerator of H(p, q), since the relationship between T_n and E_n is not linear. However, if the negative is contact copied onto another film, the transmission can be made proportional to the original exposure. The exposure on the second film (referred to as a positive transparency) is proportional to T_n. Applying Equations 8 and 9, we have

$$T_p = C_1 E_n^{(\gamma_n \gamma_p/2)} \tag{12}$$

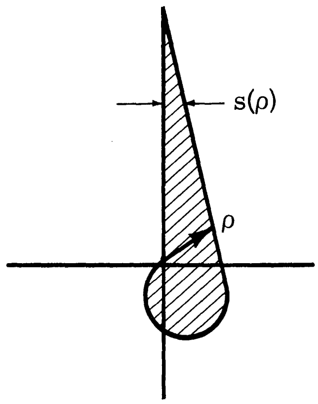

FIGURE 7. SECTOR OF CIRCLE USED TO GENERATE LOW-FREQUENCY REJECTION FILTERS

where T_p is the specular amplitude transmission of the positive

$\gamma_n\gamma_p$ is the specular γ-product of the process

If we require $\gamma_n\gamma_p = 2$, and make E_n proportional to the amplitude of the numerator, we realize the numerator of H(p, q). By placing the two transparencies in contact, we realize the entire filter for nonnegative H(p, q).

5.2. REALIZATION OF A REAL FILTER FUNCTION

If H(p, q) is real, its values lie on the real axis in the complex plane, with $|H(p, q)| \leq 1$. We can realize the negative values of H(p, q) by multiplying its magnitude by a phase function which delays the the light by $\lambda/2$. At the Institute of Science and Technology this is done by film reliefing. When certain films are exposed and bleached, depressions are left in the emulsion. The transparency is immersed in a cell (Figure 8) filled with a liquid whose refractive index is such that the actual thickness is reduced to an optical thickness of $\lambda/2$. The equation governing the parameters is

$$t = T(n_f - n_g) \tag{13}$$

where t is the optical thickness of the depressions

T is the actual thickness of the depressions

n_f is the refractive index of liquid

n_g is the refractive index of the emulsion

The resulting phase function is placed in contact with the transparencies representing the magnitude of H(p, q) and N(p, q). All three transparencies are immersed in the liquid cell to minimize unwanted phase errors in the film base.

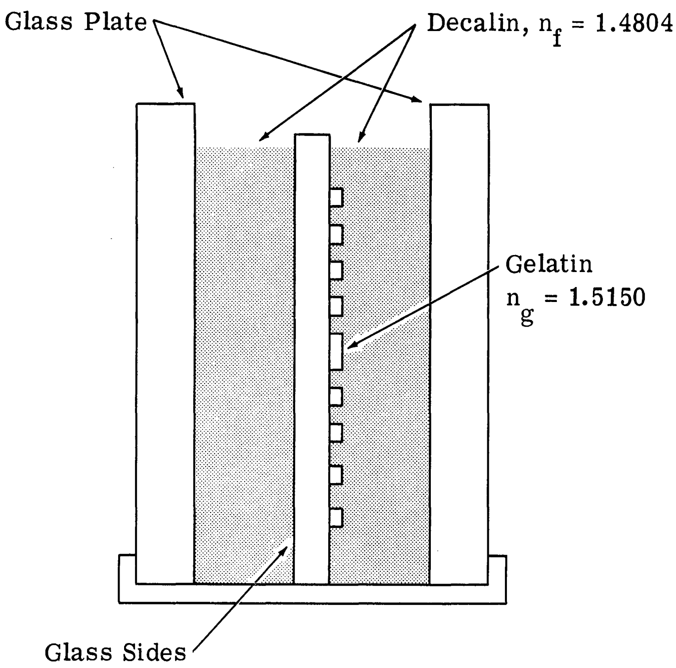

FIGURE 8. LIQUID CELL

5.3. REALIZATION OF THE COMPLEX FILTER

Since the denominator of H(p, q) can be realized as described in Section 5.1, we will concern ourselves with the problem of realizing the complex numerator of H(p, q). One problem encountered in the realization of the optimum filter is the determination of both the amplitude and phase of

$$S(p, q) = \iint_{-\infty}^{\infty} s(x, y) \exp j(px + qy)\, dx\, dy$$

One cannot merely use a spherical lens to take the Fourier transform of s(x, y), as described in Appendix B, because any physical detector measures only the intensity of S(p, q), not its phase. The second problem is to realize S(p, q) after the analysis. Since the phase function is continuous, the reliefing technique described has little value because it requires a continuous reliefing process, which is almost impossible to construct in the two-dimensional case.

We will now describe a method of analysis that leads directly to the realization of the complex conjugate of the signal spectrum. A Mach-Zehnder interferometer can be used to determine the phase in a distribution of light by combining that distribution with a reference wave whose amplitude and phase distributions are known. This interferometer is modified for our purposes as shown in Figure 9.

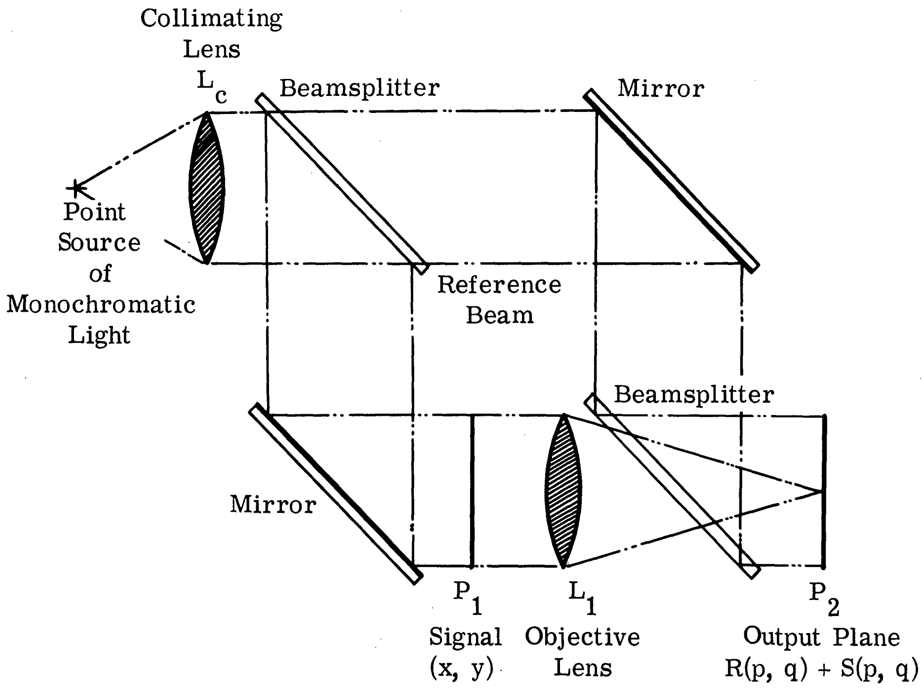

FIGURE 9. MODIFIED MACH-ZEHNDER INTERFEROMETER

The signal s(x, y) whose Fourier transform is to be found is inserted in one beam of the interferometer with a spherical lens. The lens effects the Fourier transform of s(x, y) at its back focal plane, outside the interferometer. A phase delay is placed in the reference beam to maintain temporal coherence. If we temporarily neglect aberrations in the interferometer, the observed output in the back focal plane of the lens is

$$\begin{aligned} G(p, q) &= |R(p, q) + S(p, q)|^2 \\ &= |R(p, q)|^2 + |S(p, q)|^2 + \overline{R(p, q)}\, S(p, q) + R(p, q)\, \overline{S(p, q)} \end{aligned} \tag{14}$$

where

$$R(p, q) = |R(p, q)| \exp j\phi(p, q)$$

is the light coming from the reference beam, and

$$S(p, q) = |S(p, q)| \exp j\theta(p, q)$$

is the signal spectrum. We can rewrite Equation 14 as

$$\begin{aligned} G(p, q) &= |R(p, q)|^2 + |S(p, q)|^2 + 2\mathrm{Re}\left[R(p, q)\, \overline{S(p, q)}\right] \\ &= |R(p, q)|^2 + |S(p, q)|^2 + 2|R(p, q)||S(p, q)| \cos\, [\phi(p, q) - \theta(p, q)] \end{aligned} \tag{15}$$

Both the amplitude and phase of R(p, q) could be adjusted to determine $\theta(p, q)$; but since the phase information of $\overline{S(p, q)}$ is contained in G(p, q), a nonnegative function, we will show how G(p, q) can be recorded on photographic film to realize the optimum filter.

The film is exposed so that its transmission is proportional to G(p, q). If we combine this film with the film on which 1/N(p, q) is realized, the transmission of the combination is

$$\frac{G(p, q)}{N(p, q)} = \frac{|R(p, q)|^2 + |S(p, q)|^2}{N(p, q)} + \frac{\overline{R(p, q)}\, S(p, q)}{N(p, q)} + \frac{R(p, q)\, \overline{S(p, q)}}{N(p, q)} \tag{16}$$

Suppose we require $|R(p, q)|$ to be a constant and $\phi(p, q)$ to be linear in (p, q); then

$$\frac{G(p, q)}{N(p, q)} = A(p, q) + \overline{H(p, q)}\, e^{-j(bp+cq)} + H(p, q)\, e^{j(bp+cq)} \tag{17}$$

where $A(p, q) = \dfrac{|R(p, q)|^2 + |S(p, q)|^2}{N(p, q)}$

$H(p, q) = \dfrac{k\overline{S(p), q)}}{N(p, q)}$

b, c are constants

Thus, the third term of Equation 17 is the desired filter function multiplied by a linear phase factor. The problem is to separate this term from the other two terms. This can be accomplished by inserting the filter represented by Equation 17 into the optical system (Figure 4) at plane P_2. Lens L_2 performs the separation of the three terms in the output by taking the transform of the light distribution in P_2; i.e.,

$$\text{output} = \frac{1}{4\pi^2} \iint_{-\infty}^{\infty} F(p, q) \frac{G(p, q)}{N(p, q)} e^{j(px+qy)}\, dp\, dq \tag{18}$$

Substituting Equation 17 in Equation 18, we have

$$\begin{aligned} \text{output} = {} & \frac{1}{4\pi^2} \iint_{-\infty}^{\infty} F(p, q)\, A(p, q)\, e^{j(px+qy)}\, dp\, dq \\ & + \frac{1}{4\pi^2} \iint_{-\infty}^{\infty} F(p, q)\, \overline{H(p, q)}\, e^{j[(x-b)p+(y-c)q]}\, dp\, dq \\ & + \frac{1}{4\pi^2} \iint_{-\infty}^{\infty} F(p, q)\, H(p, q)\, e^{j[(x+b)p+(y+c)q]}\, dp\, dq \end{aligned} \tag{19}$$

The first term of Equation 19, which appears on the optical axis, is of no particular interest. Nor, in this discussion, is the second term, which appears at $x = b$, $y = c$. The third term is $r(x + b, y + c)$, where $r(x, y)$ is defined by Equation 5 and is exactly the output expected from an optimum filter. This term appears with its center displaced from the optical axis by an amount $x = -b$, $y = -c$. At this point it will be convenient to set $c = 0$, since it is arbitrary; but in order to avoid overlap of the three outputs the value of b must be such that $b \geq A$, where A is the length of the signal in the x direction. The fact that this output occurs off axis by a distance $x = -b$ is not important, since the output sensor can be located properly to detect it.

In passing, a comment will be made on the significance of the second term of Equation 19. If $N(p, q) = N$ for all (p, q), we saw that the third term could be written as a cross-correlation integral (for $c = 0$); i.e.,

$$r(x + b, y) = \iint_{-\infty}^{\infty} f(u, v)\, \overline{s(x + b + u, y + v)}\, du\, dv \tag{20}$$

The second term of Equation 19 can then be written as a convolution integral, i.e.,

$$r(x - b, y) = \iint_{-\infty}^{\infty} f(u, v)\, s(x - b - u, y - v)\, du\, dv \tag{21}$$

Thus, when $N(p, q)$ is uniform, the cross-correlation and convolution of the signal with the input function are both displayed in the output plane.

If the mirrors or beam splitters in the interferometer have aberrations, the effects expressed in Equation 19 appear, and may degrade the output somewhat. The aberrations in the signal analysis beam can be neglected, because the signal is usually small compared to the aperture of the interferometer. Denote the aberrations in the reference beam by $\exp j\Psi(p, q)$. This aberration can be carried through the analysis to get (for the term of interest)

$$r(x + b), y = \frac{1}{4\pi^2} \iint_{-\infty}^{\infty} F(p, q)\, H(p, q)\, e^{j\Psi(p, q)}\, e^{j[(x+b)p+qy]}\, dp\, dq \tag{22}$$

By use of the convolution theorem, this term can be written as

$$r(x + b, y) = f(x, y) * h(x, y) * \psi(x, y)$$

where $\psi(x, y)$ is the transform of $\exp j\Psi(p, q)$. But $\psi(x, y)$ is exactly the same form as the impulse response of a lens having the aberrations $\exp j\Psi(p, q)$. Equation 22 is the output of a perfect system as "seen" by a lens with aberrations equal to $\Psi(p, q)$. It is apparent that a good quality interferometer is needed if r(x, y) has high-frequency content. (Aberrations in the various lenses can be treated in the same way as imperfections in the interferometer.)

There is an alternative optical system which can be used in place of the interferometer to realize G(p, q). In that system, shown in Figure 10, lens L_1 collimates a point source of monochromatic light. The signal is placed in one part of the beam with the necessary phase delay. (If the source has sufficient temporal coherence, the phase delay in these systems can be discarded.) Lens L_2, placed in the other part of the beam, focuses the light to a point in P_2 at a distance b from the center of the signal. Lens L_3 simultaneously takes the Fourier transform of the signal and supplies the reference wave. The reference wave automatically has a linear phase component equal to $\phi(p, q) = bp$, and the light distribution in plane P_2 is identical to that given by Equation 14.

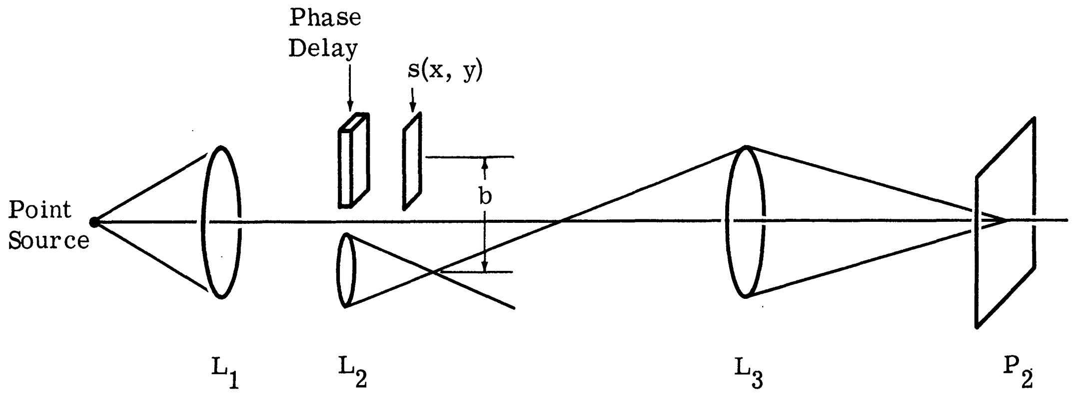

FIGURE 10. ALTERNATIVE OPTICAL SYSTEM FOR REALIZING COMPLEX FILTERS

6
SOME NOTES ON THE PERFORMANCE OF MATCHED FILTERS

6.1. CHANGE IN THE SCALE OF THE SIGNAL

We will evaluate the performance of a filter matched to a signal when the input is the signal with a change in scale. We will assume white Gaussian noise statistics.

Let s(x, y) denote the signal for which the filter was optimized, and let s(mx, my) be the input signal. Then, from Equation 5, the output of the filter is

$$r(x, y) = \frac{1}{4\pi^2} \iint_{-\infty}^{\infty} S(p, q)\, H(p, q)\, e^{j(px+qy)}\, dp\, dq$$

when the input signal is s(x, y). The output when s(mx, my) in the input is denoted by $r_m(x, y)$. We take as a measure of the change in performance of the filter

$$R = \left.\frac{|r(x, y)|^2}{|r_m(x, y)|^2}\right|_{x=y=0} = \frac{\left|\frac{1}{4\pi^2}\iint_{-\infty}^{\infty} S(p, q)\, H(p, q)\, dp\, dq\right|^2}{\left|\frac{1}{4\pi^2}\iint_{-\infty}^{\infty} \frac{1}{m^2} S(p/m, q/m)\, H(p, q)\, dp\, dq\right|^2} \tag{23}$$

Applying the Schwarz inequality to both numerator and denominator and noting that the equality holds in the numerator by Equation 3, we have

$$R \geq \frac{\iint_{-\infty}^{\infty} |S(p, q)|^2\, dp\, dq}{\iint_{-\infty}^{\infty} \left|\frac{1}{m^2} S(p/m, q/m)\right|^2 dp\, dq} \geq m^2$$

where m is the scaling factor.

6.2. CHANGE IN THE ORIENTATION OF THE SIGNAL

We wish to find some basis for evaluating the performance of a filter matched to a certain signal when the input is the same signal with a different orientation. The output of the system is conveniently expressed in polar coordinates as

$$r_{sh}(\rho, \gamma) = \int_0^{\infty} \int_0^{2\pi} s(r, \theta)\, h(r + \rho, \theta + \gamma) r\, dr\, d\theta \tag{24}$$

Considered as a function of ρ, the output is a maximum at $\rho = 0$. To investigate the effect of signal orientation on the output, we consider the normalized function

$$f(\gamma) = \frac{r_{sh}(\gamma)}{r_{sh}(0)} \tag{25}$$

For signals which are nearly rotationally symmetric, $f(\gamma) \approx 1$ for all γ. Our first task is to find a measure of the degree of nonrotational symmetry (termed orientativeness) or the signal. We begin by forming the function

$$g(r, \theta) = s(r, \theta) - k(r)$$

where

$$k(r) = \frac{1}{2\pi}\int_0^{2\pi} s(r, \theta)\, d\theta$$

Thus, $g(r, \theta)$ represents a measure of the difference between the signal and a function which has rotational symmetry. We then evaluate

$$R_{gh}(\gamma) = R_{sh}(\gamma) - R_{kh}(\gamma)$$

But

$$R_{kh}(\gamma) = \frac{1}{2\pi}\int_0^{2\pi}\int_0^{\infty}\int_0^{2\pi} s(r, \phi)\, h(r, \theta + \gamma)\, r\, dr\, d\theta\, d\phi$$

Since we integrate over all θ, we can write $\theta + \gamma = \alpha$ and let $\alpha - \phi = \beta$, so that

$$R_{kh} = \frac{1}{2\pi}\int_0^{2\pi}\left[\int_0^{\infty}\int_0^{2\pi} s(r, \phi)\, h(r, \phi + \beta) r\, dr\, d\phi\right] d\beta$$

$$= \mathrm{Ave}\left[R_{sh}(\beta)\right] \tag{26}$$

and

$$R_{gh}(\gamma) = R_{sh}(\gamma) - \mathrm{Ave}\left[R_{sh}(\gamma)\right]$$

We now look at the normalized function

$$f_1(\gamma) = \frac{R_{gh}(\gamma)}{R_{gh}(0)} \tag{27}$$

and define the "orientativeness" or the signal to be

$$\mathrm{Or} = \frac{\pi}{\gamma_c} - 1 \qquad 0 \le \gamma_c \le \pi$$

where γ_c is the angle for which $f_1(\gamma) = C$, $0 \le C \le 1$. By constructing the fu one can always find a γ for which $f_1(\gamma) = C$ for any signal. The function $f_1(\gamma)$ is now the measure of the performance of a filter matched to a signal when the input is a signal which has undergone a change of orientation. This result is highly dependent on the shape of the signal, whereas the result of Section 6.1 was not.

7
EXPERIMENTAL RESULTS

A few experimental results will serve to illustrate the theory of spatial filtering and indicate the potential to be expected when complex filters can be realized. A practical result of realizing complex filters by the technique described in Section 5.3 is that the noise rejection capability is better than that of conventional filters, since the minimum transmission of films is not zero when the γ-product is fixed, and some noise passes through the filter. In the method described in Section 5.3, the carrier frequency is recorded only for those values of (p, q) for which $S(p, q) \neq 0$. Since the noise passing through the filter where $S(p, q) = 0$ is not deviated into the output of interest, the effective transmission at those points is in effect equal to zero.

7.1. DETECTION OF SIMPLE GEOMETRICAL SHAPES

The first example presented is the detection of one of the elementary geometrical shapes shown in Figure 11. Any of the shapes could serve as the signal; we chose the small rectangle first. We realized the complex filter of this signal by the method described in Section 5.3; the output of interest is shown in Figure 12. Note that all signals with proper shape and orientation were detected simultaneously.

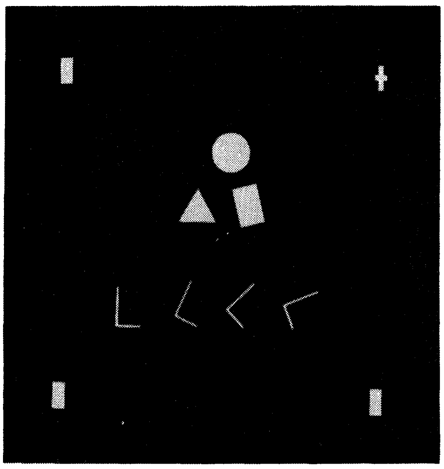

FIGURE 11. SET OF GEOMETRICAL SHAPES

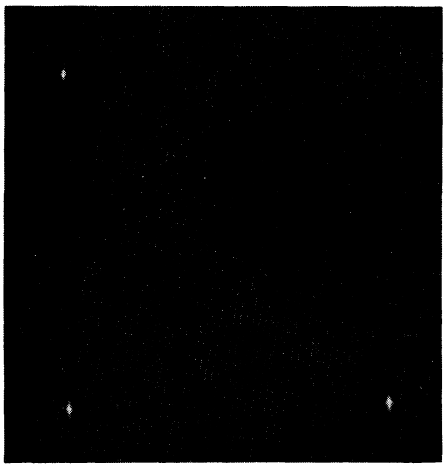

FIGURE 12. DETECTION OF RECTANGLES

The second signal selected was the "L" shape, which has a complex spectrum. The Fourier transform of the complex filter, shown in Figure 13, illustrates the fidelity with which the complex filter was realized. The light distribution in the center of the output is the transform of the first two terms of Equation 14. The L in the upper corner is the transform of the third

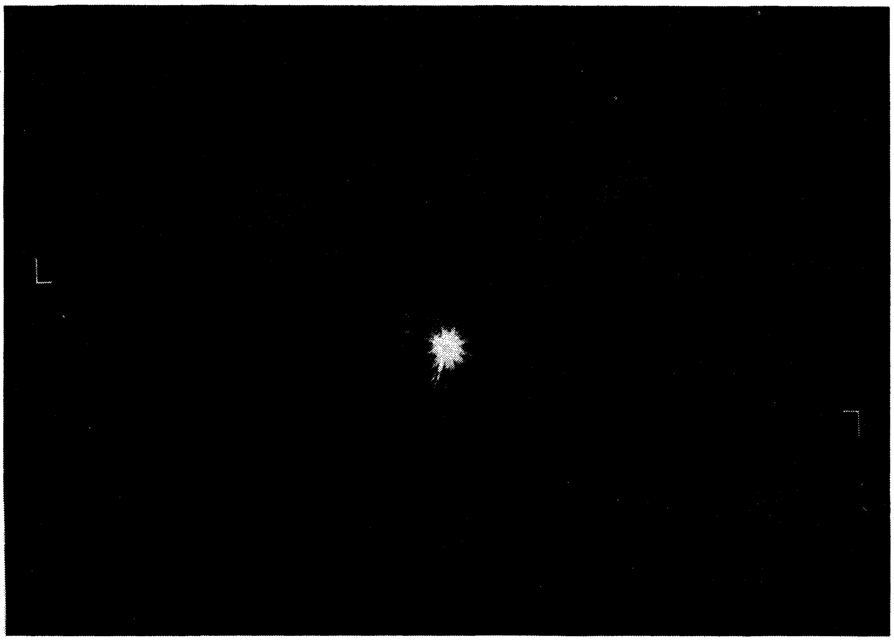

FIGURE 13. RECONSTRUCTION FROM A COMPLEX FILTER

term, and the other L is the transform of the last term. Note that these two images are inverted and reversed relative to each other, which graphically demonstrates that the Fourier transform of $[S(p, q)] = s(x, y)$ and the Fourier transform of $\overline{[S(p, q)]} = \overline{s(-x, -y)}$. Of course, since $s(x, y)$ is real, $\overline{s(-x, -y)} = s(-x, -y)$. Figure 14 shows the output, which is the cross-correlation of the "L" with the input function. Note the symmetry in the output correlation, which is a necessary feature of cross-correlation. The other L's in the input, having different orientations, do not give as large an output (cf. Section 6.2), but a rotation of the filter relative to the input would sequentially detect them. The output, which is shown for illustration in Figure 15, is the convolution of the signal with the input function. Note that it is asymmetrical, a consequence of convolution unless the signal is even.

7.2. DETECTION OF ALPHANUMERICS

The second example is the detection of alphanumerics. An interesting variation of the first example is to record the alphabet (shown in Figure 16) via its complex spectrum as the filter function. It is a simple matter to select any one of the alphanumerics as the signal to be detected and use it as the input signal. The output, when the input is the letter "g," is shown in Figure 17. Since the filter (which is the normal input function in disguise) does not have to be changed while the search is carried out, this technique suggests a method for scanning a printed page for the presence of any particular alphanumeric.

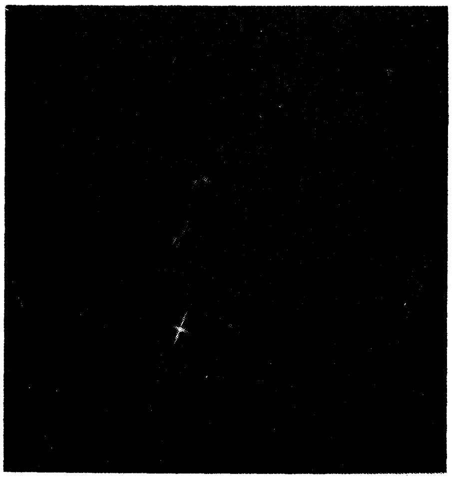

FIGURE 14. CROSS CORRELATION OF L WITH THE SET OF SHAPES SHOWN IN FIGURE 11

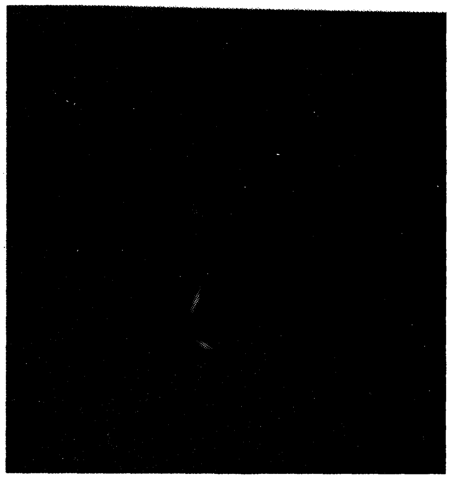

FIGURE 15. CONVOLUTION OF L WITH THE SET OF SHAPES SHOWN IN FIGURE 11

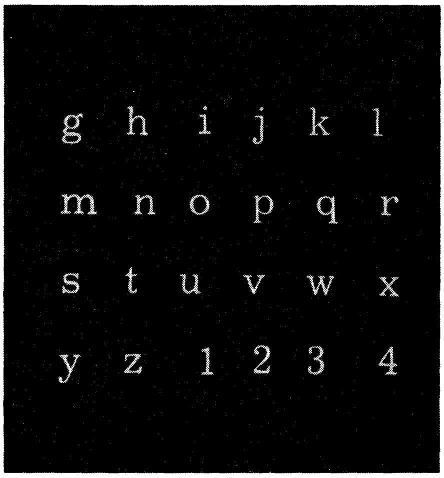

FIGURE 16. SET OF ALPHANUMERICS

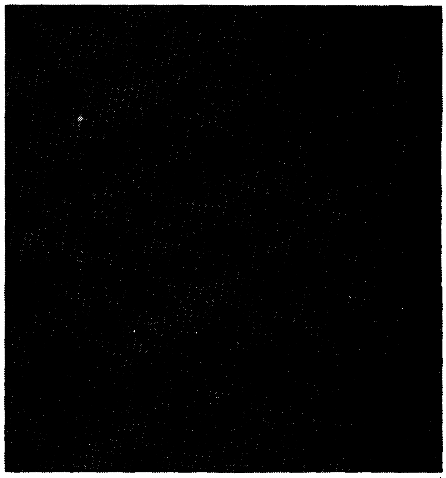

FIGURE 17. DETECTION OF LETTER g

7.3. DETECTION OF AN ISOLATED SIGNAL IN RANDOM NOISE

In the preceding two examples the noise spectral density was uniform enough to be considered white. This final example shows the detection of a signal which is immersed in a noise background with nonuniform spectral density, and demonstrates the power of using a coherent system for signal detection.

Figure 18(a) shows a figure in a noise background. Since the noise background is predominantly low-frequency, the denominator of the filter must be realized. Figure 18(b) shows that the background noise has been completely suppressed and the signal has been detected.

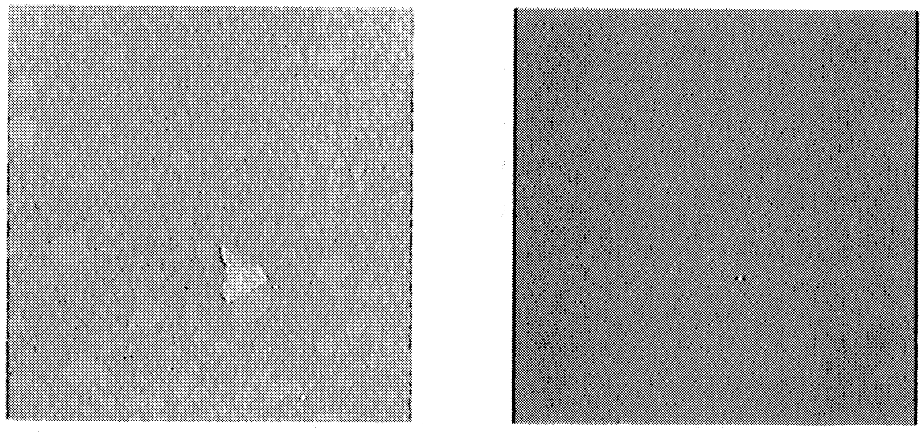

(a) (b)

FIGURE 18. DETECTION OF ISOLATED SIGNAL IN NOISE BACKGROUND. (a) Signal plus noise. (b) Detection of signal.

Appendix A

OPTIMIZATION IN PRESENCE OF MUTUALLY EXCLUSIVE NOISE

One consideration in optimum filtering of photorecords is that the noise is frequently mutually exclusive and not additive. We can consider the signal g(x, y) to be multiplied by an indicator function I(x, y), which is a random process on x, y having a known autocorrelation function. Since the desired signal is now random rather than known, the optimum filtering process is found by performing a least squares analysis. A block diagram describing the system is shown in Figure 19.

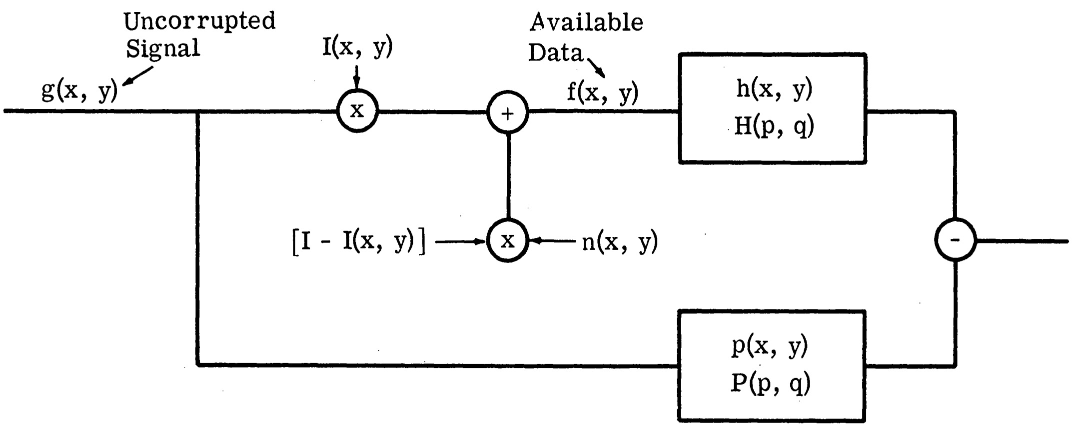

FIGURE 19. PROCESSING SYSTEM WHEN MUTUALLY EXCLUSIVE NOISE IS PRESENT

I(x, y) is an indicator function taking on values (0, 1) and is an approximation to a mutually exclusive noise function. P(p, q) is some operation on G(p, q); in our case P(p, q) = 1 for all (p, q) of interest. The problem is to find a filter function H(p, q) which will minimize the expected value of $|\epsilon|^2$.

We will continue the analysis for one dimension; the two-dimensional extension is obvious. We write

$$E\left[\epsilon(x+u)\,\overline{\epsilon(x)}\right] = R_\epsilon(u)$$

which is the autocorrelation function of the error term (E is the expected value). $R_\epsilon(u)$ will be expressed in terms of the usual autocorrelation functions of g(x), f(x), and n(x), and it can readily be seen that $E(|\epsilon|^2) = R_\epsilon(0)$.

A useful relationship between $R_\epsilon(u)$ and its spectral density is given by

$$R_\epsilon(u) = k \int_{-\infty}^{\infty} S_\epsilon(p)\, e^{-jpu}\, dp$$

and we note immediately that

$$R_\epsilon(0) = E[|\epsilon|^2] = k \int_{-\infty}^{\infty} S_\epsilon(p)\, dp$$

Since $S_\epsilon(p)$ is the Fourier transform of an autocorrelation function, $S_\epsilon(p) \geq 0$ for all p, and we can minimize $R_\epsilon(0)$ by minimizing $S_\epsilon(p)$. To find $S_\epsilon(0)$ we write

$$\epsilon(x) = f(x) * h(x) - g(x) * p(x)$$

where * denotes convolution. Then

$$\begin{aligned} R_\epsilon(u) &= E[\epsilon(x+u)\,\overline{\epsilon(x)}] \\ &= E[f(x+u) * h(x+u) - g(x+u) * p(x+u)]\,[\overline{f(x)} * \overline{h(x)} - \overline{g(x)} * \overline{p(x)}] \end{aligned}$$

$$\begin{aligned} R_\epsilon(u) &= R_f(x) * h(x) * \overline{h(-x)} + R_g(x) * p(x) * \overline{p(-x)} \\ &\quad - R_{gf}(x) * h(x) * \overline{p(-x)} - R_{fg}(-x) * p(x) * \overline{h(-x)} \end{aligned}$$

Taking Fourier transforms of both sides and using the result that

$$\mathcal{F}[R_y(x) * h(x) * \overline{p(-x)}] = S_y(p)H(p)\overline{P(p)}$$

we have

$$S_\epsilon(p) = S_f(p)|H(p)|^2 + S_g|P(p)|^2 - S_{gf}(p)H(p)\overline{P(p)} - \overline{S_{gf}(p)}P(p)\overline{H(p)}$$

Complete the square in H(p) to get

$$S_\epsilon(p) = \left| S_f(p)^{1/2} H(p) - \frac{S_{gf}(p)P(p)}{S_f(p)^{1/2}} \right|^2 + S_g(p)|P(p)|^2 - \frac{|S_{gf}(p)P(p)|^2}{S_f(p)}$$

where $S_f(p)$ is the spectral density of the available data

$S_g(p)$ is the spectral density of the signal

$S_{gf}(p)$ is the cross-spectral density of the signal with available data

P(p) is the desired operation on the signal

H(p) is the filter function which is being optimized

We can choose H(p) to minimize $S_\epsilon(p)$. It is apparent that H(p) has no influence on the last two terms of $S_\epsilon(p)$; therefore we take

$$H(p) = \frac{S_{gf}(p)P(p)}{S_f(p)}$$

which minimizes $S_\epsilon(p)$ and therefore minimizes $E(|\epsilon|^2)$. To recover the signal with minimum error, we let P(p) = 1 for all p, and we have

$$H(p) = \frac{S_{gf}(p)}{S_f(p)}$$

To get this into a useful form, we write $S_{gf}(p)$ and $S_f(p)$ in terms of the statistics of the input functions. To determine $S_f(p)$, we have

$$f(x) = n(x)\,[1 - I(x)] + g(x)I(x)$$

and

$$R_f(x) = E[f(x+u)f(x)] = (1 - 2a)\,R_n(x) + R_n(x)\,R_I(x)$$
$$+ R_g(x)R_I(x) + 2abc - 2bcR_I(x)$$

Take Fourier transform of both sides to get

$$S_f(p) = (1 - 2a)S_n(p) + S_n(p) * S_I(p) + S_g(p) * S_I(p) + 2abc\delta(p) - 2bcS_I(p)$$

where $a = E[I(x)]$

$b = E[g(x)]$

$c = E[n(x)]$

$\delta(p) = C$ sinc kA (A = aperture of optical system)

A similar analysis for $S_{gf}(p)$ gives

$$S_{gf}(p) = aS_g(p) + (1 - a)bc\delta(p)$$

Thus we can now write the optimum filter in terms of the known statistics of the input data and the indicator function, as follows:

$$H(p) = \frac{aS_g(p) + (1 - a)\,bc\delta(p)}{(1 - 2a)S_n(p) + S_g(p) * S_I(p) + S_n(p) * S_I(p) + 2abc\delta(p) - 2bcS_I(p)}$$

This result shows that, in general, the best filtering operation is to attenuate the spectrum heavily where there is little signal energy, and vice-versa. More precise information on H(p) will be obtainable if the autocorrelation function of I(x) is known.

Appendix B
THE FOURIER TRANSFORMING PROPERTY OF LENSES

B. 1. DERIVATION OF THE FOURIER TRANSFORM RELATIONSHIP

The theory outlined in Section 2 of this report is based on the assumption that a spherical lens can effect the two-dimensional Fourier transform of a complex distribution of light. It is also asserted that the transform relationship holds, to within a phase factor, for a wide variety of positions of the lens relative to the input transparency, so that we can cascade lenses to take successive transforms. The analysis in this appendix is in one dimension; the extension to two dimensions is obvious, though not simple.

We begin by assuming that a transparency with complex transmission f(x) is placed in plane P_1 at a distance d from the lens in plane P_2 (see Diagram 1). Although the transform relationship is found with far less effort if d = f, the results are not general enough to apply in evaluating the performance of combinations of lenses. We proceed from the application of Kirchoff's formulation of Huygens' principle [7], which indicates that the disturbance at a point in P_2 due to a disturbance in P_1 is given by

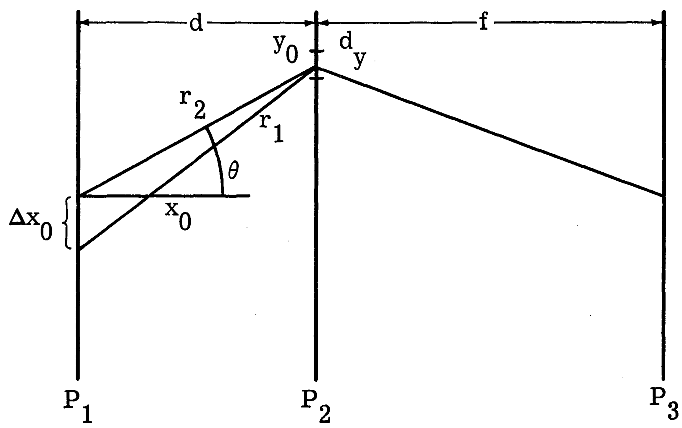

DIAGRAM 1

$$\sqrt{-\frac{j}{\lambda}}\,\frac{Af(x_o)\,e^{jkr}}{\sqrt{r}}\,\frac{(1+\cos\theta)}{2}\,\Delta x_o \tag{28}$$

where λ is the wavelength of light

A is the amplitude of illumination at point x_o

r is the distance from x_o to y_o

θ is the obliquity angle, i.e., the angle from x_o to y_o measured from the optical axis

$f(x_o)$ is the transmission of transparency at $x = x_o$

$k = 2\pi/\lambda$

The incoming illumination is $E(x) = A(x) \exp j\phi(x)$; usually $A(x)$ and $\phi(x)$ are constant. Since the exact value of $\phi(x)$ is unimportant, we can set it equal to zero and regard it as the reference phase. The total contribution at the point y_o is

$$g(y) = \sqrt{-\frac{j}{\lambda}}\, A \int_{P_1} \frac{f(x) \exp(jkr)(1 + \cos\theta)}{2\sqrt{r}} dx \tag{29}$$

The obliquity factor is usually neglected by assuming that θ remains small throughout the integration. Though this may be true when $d \geq f$, it is not true when $d \to 0$, and a better reason for neglecting the obliquity factor must be sought.

Consider the effect of the contribution from the points in a small region in P_1 on a given point in P_2. If $|r_2 - r_1| >> \lambda$, the contribution at y_o averages to zero if $f(x_2) \simeq f(x_1)$. Thus we can determine the maximum permissible value of θ as a function of d and the frequency content of f(x). In terms of x, y, and d, the condition that $|r_2 - r_1| >> \lambda$ implies that $\left|\sqrt{d_1^2 + (x - y)^2} - \sqrt{d^2 + (x + \Delta x - y)^2}\right| >> \lambda$, or that $|2x\Delta x + (\Delta x)^2 - 2y\Delta x| >> 2\lambda d$.

Neglecting $(\Delta x)^2$ with respect to the other terms, we have

$$\Delta x >> \frac{\lambda d}{x - y} \tag{30}$$

Suppose we agree that the obliquity factor can be neglected if

$$\frac{1 + \cos\theta}{2} \geq 0.99$$

which implies that $\tan\theta \leq 0.20$. But $\theta = \arctan(x - y)/d$, so that

$$\frac{x - y}{d} \leq 0.20 \tag{31}$$

and from Equation 30 we have that $\Delta x >> \frac{\lambda}{0.20}$. Since Δx is the distance over which f(x) must not vary appreciable, the highest allowable frequency in f(x) is

$$p_{max} = 1/\Delta x << 0.20/\lambda << 375 \text{ l/mm}$$

Since the highest frequency encountered in typical input signals is approximately 30 to 50 l/mm, it seems safe to neglect the obliquity factor. Note that this analysis makes no restriction on the relative aperture of the system, the permissible field of view, or the value of d. These restrictions comprise the reasons usually cited for neglecting this factor.

If we ignore the obliquity factor, the light distribution in P_2 is

$$g(y) = \sqrt{-\frac{j}{\lambda}}\, A \int_{P_1} \frac{f(x)}{\sqrt{r}} e^{jkr} dx \tag{32}$$

Expanding $r = \sqrt{d^2 + (x - y)^2}$ by the binomial theorem, we have

$$r = d\left[1 + \frac{1}{2}\left(\frac{x - y}{d}\right)^2 - \frac{1}{8}\left(\frac{x - y}{d}\right)^4, \ldots\right] \tag{33}$$

From our previous assumption, $(x - y)/d \leq 0.2$, so that we need retain only the first two terms of Equation 33. Since the $\sqrt{r}$ term in the denominator is relatively insensitive to the small variations in $(x - y)^2/d^2$ over the region of integration, we set $r = d$ and take it outside the integral. Also the phase term exp (jkd) is constant and can be dropped from the analysis. The lens at P_2 is represented by the phase factor $\exp[-j(ky^2/2f)]$, where f is the focal length of the lens. The P_2 plane can be considered the back principal plane of the lens. We will proceed from P_2 to P_3 in the same way as from P_1 to P_2. The total contribution at a point ξ in P_3 is

$$F(\xi) = \frac{-jA}{\lambda\sqrt{df}} \int_{P_1} dx \int_{P_2} dy\, f(x) \exp\left[j\left(\frac{k}{2f}\right)(y - \xi)^2\right] \times \exp\left(j\left(\frac{k}{2f}\right)y^2\right)\exp\left[j\left(\frac{k}{2f}\right)(y - \xi)^2\right] \tag{34}$$

Looking at the exponent only, we have

$$\text{exponent} = j\frac{k}{2d}(x^2 - 2xy + y^2) - j\frac{k}{2f}y^2 + j\frac{k}{2f}(y^2 - 2y\xi + \xi^2) \tag{35}$$

Let $f/d = m$, and complete the square in Equation 35 to get

$$\text{exponent} = j\frac{k}{2f}[\sqrt{m}\, y - (\sqrt{m}\, x + \xi)]^2 - j\frac{k}{f}(y\xi - \sqrt{m}\, y\xi) - j\frac{k}{f}(\sqrt{m}\, x\xi) \tag{36}$$

Substituting Equation 36 in Equation 34, we get

$$F(\xi) = \frac{-jA}{\lambda\sqrt{df}} \int_{P_1} dx \int_{P_2} dy\, f(x) \exp\left\{j\frac{k}{2f}[\sqrt{m}\, y - (\sqrt{m}\, x + \xi)]^2\right\}$$

$$\times \exp\left(-j\frac{k}{f}\sqrt{m}\, x\xi\right) \exp\left\{-j\frac{k}{f}[(1 - \sqrt{m})\, y\xi)\right\}$$

$$= -\frac{jA}{\lambda\sqrt{df}} \int_{P_1} dx\, f(x) \exp\left(-j\frac{k}{f}\sqrt{m}\, x\xi\right) v(x, \xi) \tag{37}$$

where

$$v(x, \xi) = \int_{P_2} dy \exp\left\{j\frac{k}{2f}[\sqrt{m}\, y - (\sqrt{m}\, x + \xi)]^2\right\} \exp\left\{-j\frac{k}{f}[(1 - \sqrt{m})\, y\xi]\right\} \tag{38}$$

Evaluating $v(x, \xi)$, we let $\sqrt{m}\, y - (\sqrt{m}\, x + \xi) = p$, and we have

$$v(x, \xi) = \frac{1}{\sqrt{m}} \int_{l.l.}^{u.l.} dp \exp\left[-j\frac{k}{f}\left(\frac{1 - \sqrt{m}}{\sqrt{m}}\right)\xi\,(p + \sqrt{m}\, x + \xi)\right] \exp\left(j\frac{k}{2f}p^2\right) \tag{39}$$

where

$$\text{u.l.} = \sqrt{m}\,A - (\sqrt{m}\,x + \xi)$$

$$\text{l.l.} = -\sqrt{m}\,A - (\sqrt{m}\,x + \xi)$$

$$2A = \text{aperture in } P_2$$

We can pass the phase factor $\exp\left[-j\frac{k}{f}\left(\frac{1-\sqrt{m}}{\sqrt{m}}\right)\xi\,(\sqrt{m}\,x + \xi)\right]$ through the integral, since it is not a function of the variable of integration. Thus

$$F(\xi) = \frac{-jA\exp\left[-j\frac{k}{f}\left(\frac{1-\sqrt{m}}{\sqrt{m}}\right)\xi^2\right]}{\lambda\sqrt{df\,m}} \int_{P_1} dx\, f(x)\exp\left[-j\frac{k}{f}\sqrt{m}\,x\xi\right] \times \exp\left[-j\frac{k}{j}\left(\frac{1-\sqrt{m}}{\sqrt{m}}\right)\sqrt{m}\,x\xi\right] b(x,\xi) \tag{40}$$

where

$$b(x,\xi) = \int_{\text{l.l.}}^{\text{u.l.}} \exp\left[j\frac{k}{2f}p^2\right]\exp\left[-j\frac{k}{f}\left(\frac{1-\sqrt{m}}{\sqrt{m}}\right)\xi\,p\right]dp \tag{41}$$

Note that part of the phase term in the integrand of Equation 4 cancels out, leaving

$$F(\xi) = \frac{-jA\exp\left[-j\frac{k}{f}\left(\frac{1-\sqrt{m}}{\sqrt{m}}\right)\xi^2\right]}{\lambda\sqrt{df\,m}} \int_{P_1} dx\, f(x)\exp\left(-j\frac{k}{f}x\xi\right) b(x,\xi) \tag{42}$$

If $b(x, \xi) = k$ for all (x, ξ) of interest, and if $m = 1$, we have an exact Fourier transform relationship between $F(\xi)$ and $f(x)$. Further, the integral in Equation 42 is independent of m, which is to be expected since the scale of $F(\xi)$ is not a function of m. (The manner in which the phase term depends on m will be discussed after $b(x, \xi)$ is evaluated.) Since Equation 41 determines the validity of the Fourier transform relationship, we modify $b(x, \xi)$ to a Fresnel integral, which is easier to evaluate than the form given. Completing the square in the exponent, we get

$$b(x,\xi) = \exp\left[-j\frac{k}{2f}\left(\frac{1-2\sqrt{m}+m}{m}\right)\xi^2\right]\int_{\text{l.l.}}^{\text{u.l.}} \exp\left\{j\frac{k}{2f}\left[p - \left(\frac{1-\sqrt{m}}{\sqrt{m}}\right)\xi\right]^2 dp\right\} \tag{43}$$

Change variables by letting

$$p - \left(\frac{1-\sqrt{m}}{\sqrt{m}}\right)\xi = \sqrt{\pi f/k}\,v$$

so that

$$b(x,\xi) = \sqrt{\pi f/k}\exp\left[-j\frac{k}{2f}\left(\frac{1-2\sqrt{m}+m}{m}\right)\xi^2\right]\int_{\text{l.l.}}^{\text{u.l.}} \exp\left[j(\pi/2)v^2\right]dv \tag{44}$$

where the new upper and lower limits are

$$\text{u.l.} = \sqrt{\frac{2m}{\lambda f}}\,[A - x - \xi/m] \tag{45a}$$

$$\text{l.l.} = \sqrt{\frac{2m}{\lambda f}}\,[-A - x - \xi/m] \tag{45b}$$

Before evaluating Equation 44, we will discuss the general behavior of the function

$$F(u) = \int_{-(A+u)}^{A-u} \exp[j(\pi/2)v^2]\,dv$$

which is a Fresnel integral in its standard form. The evaluation of F(u) cannot be given in a closed form, but the function is tabulated extensively. If the function is written as

$$F(u) = \left[\int_{-(A+u)}^{A-u} \cos(\pi/2)v^2\,dv + j\int_{-(A+u)}^{A-u} \sin(\pi/2)v^2\,dv\right]$$

$$= x + jy \tag{46}$$

one can use a curve known as a Cornu spiral, which plots the first integral against the second (see Figure 20). Values of u are read along the curve, and the corresponding values of x and y are read from the coordinate axis. The magnitude of F(u) is found in the usual way. It can be seen from the curve that F(u) has its greatest change in value near $|u| = A$, so that we have as an approximation

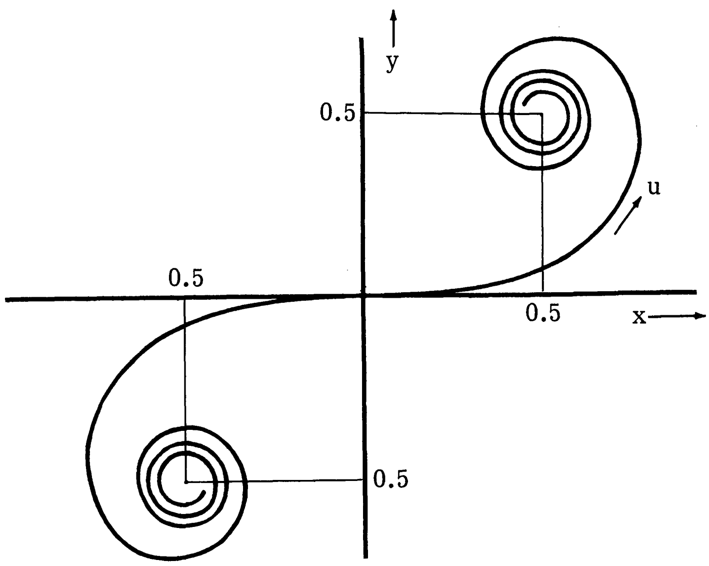

FIGURE 20. CORNU SPIRAL

$$F(u) = \sqrt{2} \qquad |u| < A$$

$$= 0 \qquad |u| > A$$

In Equation 44, $u = x + \frac{\xi}{m}$, and the factor $\sqrt{\frac{2m}{\lambda f}}$ in both limits represents a scaling factor. We first look at the case in which $A >> |x + \frac{\xi}{m}|$. Then the integral reduces to $\sqrt{2}$ and

$$b(x, \xi) = \sqrt{2\pi f/k} \exp\left[-j\frac{k}{2f}\left(\frac{1 - \sqrt{2m} + m}{m}\right)\xi^2\right] \tag{47}$$

which is independent of x as expected, since the given requirement is equivalent to demanding that the system is space invariant, i.e., $F(\xi)$ is not a function of the position at which the signal is found in P_1. Substituting Equation 47 in Equation 44 and simplifying, we have

$$F(\xi) = \frac{-jA}{\sqrt{\lambda f}} \exp\left[-j\frac{k}{2f}\left(\frac{1 - m}{m}\right)\xi^2\right] \int_{P_1} f(x) \exp\left[-\frac{jk}{f} x\xi\right] \tag{48}$$

Note that if the input transparency is in the front focal plane of the lens ($m = 1$) the result is an exact Fourier transform relationship. For $m < 1$, the factor $(1 - m)/m > 0$, and the quadratic phase term indicates that the lens is capable of forming a real image of f(x) to the right of the lens at a distance

$$d_1 = \frac{f}{1 - m}$$

If $m > 1$, the image is virtual and cannot be imaged to the right of the lens without the aid of a second lens.

The remaining task is to evaluate $b(x, \xi)$ for the case in which the condition $A >> (x + \frac{\xi}{m})$ is not satisfied. We want to investigate three different cases, $m \to \infty$, $m = 1$, and $m \to 0$. We can facilitate the analysis by restricting our attention to values of $x > 0$ and $\xi > 0$, since similar results will hold for $x < 0$, $\xi < 0$.

In the first case of interest, m is very large; i.e., the transparency is close to the principal plane of the lens. In this case ξ/m is very small and

$$b(x, \xi) = f(\xi) \int_{-\sqrt{2m/(\lambda f)}(A+x)}^{\sqrt{2m/(\lambda f)}(A-x)} \exp\left(j\frac{\pi}{2} v^2\right) dv \tag{49}$$

where

$$f(\xi) = \sqrt{\pi f/k} \exp\left[-j\frac{k}{2f}\left(\frac{1 - \sqrt{2m} + m}{m}\right)\xi^2\right]$$

The limit on the maximum signal aperture to satisfy space invariance is $|X| \leq A$. Hence, in order to obtain maximum system aperture, the input signal should be placed very close to the lens. A second lens is necessary to image f(x), but it can also be selected to maximize system frequency response. This is discussed more fully in Appendix B, Section 3.

In the second case to be discussed, m = 1. Then $f(\xi) = \sqrt{\pi f/k}$ and

$$b(x, \xi) = \sqrt{\frac{\pi f}{k}} \int_{-\sqrt{2/(\lambda f)}(A+x+\xi)}^{\sqrt{2/(\lambda f)}(A-x-\xi)} \exp\left(j\frac{\pi}{2}v^2\right) dv \tag{50}$$

For small x we see that $b(x, \xi)$ reaches its half-amplitude point for $|\xi| = A$ and

$$\begin{aligned} b(x, \xi) &= \sqrt{2\pi f/k} & |\xi| < A \\ &= 0 & |\xi| > A \end{aligned}$$

This is the classical result, the so-called aperture limited frequency cutoff. However, this result is valid only for small signal apertures; as the signal aperture increases, the symmetrical band pass decreases and the lens system becomes space variant.

It is almost impossible to continue this discussion without placing a limitation on the frequency content of the signal. Suppose the highest frequency of the signal is displayed at ξ_o, which corresponds to a maximum frequency of

$$p_o = \frac{2\pi\xi_o}{\lambda f} \text{ rad/mm}$$

We then find the largest range on the signal aperture which will retain space invariance. From Equation 44 we see that this condition is satisfied if

$$\begin{aligned} (x + \xi_o/m) &\leq A & \text{for } x > 0 \\ (x - \xi_o/m) &\leq -A & \text{for } x < 0 \end{aligned}$$

Thus, to have space invariance we must restrict the signal aperture such that

$$|X| < (A - \xi_o/m) \tag{51}$$

From Equation 51 it is easy to see the result for $m \to 0$. As m becomes smaller, the input signal is farther from the lens, and the allowable range on $|X|$ rapidly decreases. In those regions where $|X|$ exceeds the limitation imposed by Equation 51, the symmetrical frequency response is reduced, and the result is a space variant operation. For perfect lenses, $b(x, \xi)$ adequately describes the space variant characteristics of the lens, but aberrations usually cause the system to be space variant before Equation 51 is violated, except for small values of m.

This section presents a general discussion of the Fourier transform properties of a lens operating with coherent illumination. The generality allows a determination of the validity of the Fourier transforming property of the lens. Equation 44 relates the frequency response of a lens to the region over which it can be considered space invariant. An application of the results of this section will be used in Section B. 3, in evaluating complete lens systems.

B. 2. AN ALTERNATIVE APPROACH TO THE TRANSFORM RELATIONSHIP

If Section B.1 masks the fundamental results to be obtained from b(x, ξ), the following approach may be instructional. It is known that a δ-function is equivalent to a point source in the input plane (Diagram 2). A point source in P_1 creates a spherical wave at P_2 with radius

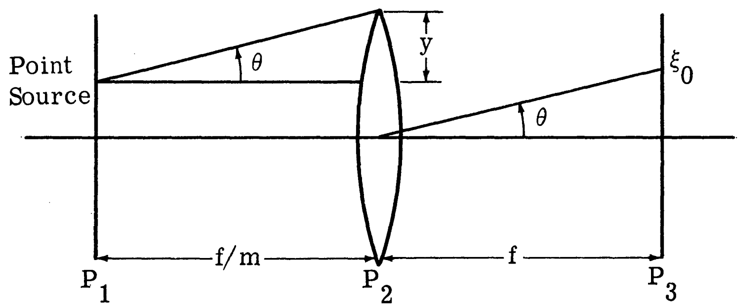

DIAGRAM 2

f/m. Each element on the wave can be considered to be a certain frequency, and if the highest frequency of the signal is $P_o = \frac{2\pi\xi_o}{\lambda f}$, we require that all the energy from that element enter the lens. Let the element representing P_o be located a distance $(x + y) \leq A$ above the optical axis. Then $\tan \theta = \frac{y}{f/m} = \frac{\xi_o}{f}$ or $y = \xi_o/m$. To get all the light from this element into the lens, we require that $(x + y) < A$ or $x < (A - \xi_o/m)$. A similar situation holds for $x < 0$; so we have $|X| < (A - \xi_o/m)$, which is Equation 51. Thus, this approach yields the same major result as the detailed analysis of b(x, ξ). The minor oscillation of b(x, ξ) is not accounted for, since diffraction effects of the lens aperture were not considered here; otherwise the results would be identical.

B.3. EVALUATION OF OPTICAL SYSTEMS

In this section, the results from Section B.1 will be used to evaluate three basic systems which perform fundamental spatial filtering operations. We will evaluate the systems on the basis of (1) the maximum frequency that the system will image for a limited region in the input plane, (2) the maximum signal aperture that can be imaged when the input signal is band-limited and the lens system operates as a space invariant system, and (3) minimum total system length. Each system will have unity magnification.

B.3.1. THREE-LENS SYSTEM. Perhaps the simplest system to analyze is the three-lens system shown in Figure 21. Lens L_1 collimates a point source, and the input transparency is placed in plane P_1 close to lens L_2. From Equation 51 we note that the maximum frequency response of lens L_2 is extremely high, but that the maximum frequency that can be imaged is limited by L_3 to $p_{max} = \frac{2\pi A}{\lambda f}$ rad/mm. The length of signal which can be imaged with space invariance when the signal is band limited to frequency p_o is

$$|x| < \left(A - \frac{p_o \lambda f}{2\pi}\right) \text{mm}$$

If lens L_2 has a focal length of 1/2 f, the total system length is 3f.

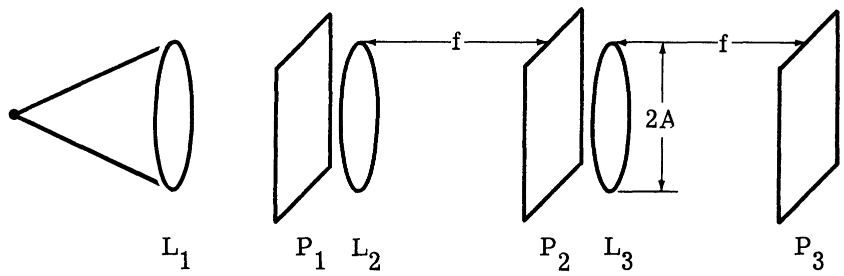

FIGURE 21. THREE-LENS SYSTEM

B.3.2. TWO-LENS SYSTEM. A two-lens system is shown in Figure 22. In this system L_1 collimates the point source and the input transparency is placed in plane P_1 at a distance 2f from L_2. Lens L_2 is the transforming lens as well as the imaging lens. The maximum frequency imaged by this system is $p_{max} = \frac{\pi A}{\lambda f}$ rad/mm. The maximum signal length to be imaged under space invariance and maximum frequency content p_o is

$$|x| < \left(A - \frac{p_o \lambda f}{\pi}\right) \text{mm}$$

The total system length is 5f.

B.3.3. ONE-LENS SYSTEM. The one-lens system shown in Figure 23 can also perform the desired operation. In this case the signal is illuminated not be a plane wave, but by a divergent wave of radius r = s - d. The frequency plane is located at a distance t from lens L_1, where t = st/(s - f). The image plane is at a distance q = df/(d - f) from lens L_1. The maximum frequency passed by the lens for small signal lengths is $p_{max} = 2\pi A/(\lambda d)$ rad/mm.

The maximum signal length which is imaged when the lens operates under a space invariant condition and the signal is limited to frequencies less than p_o will now be found. Equation 51 cannot be applied directly, because the illumination is not a plane wave and the frequency plane

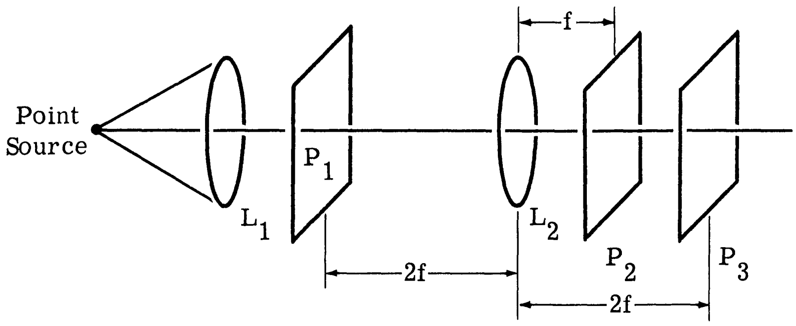

FIGURE 22. TWO-LENS SYSTEM

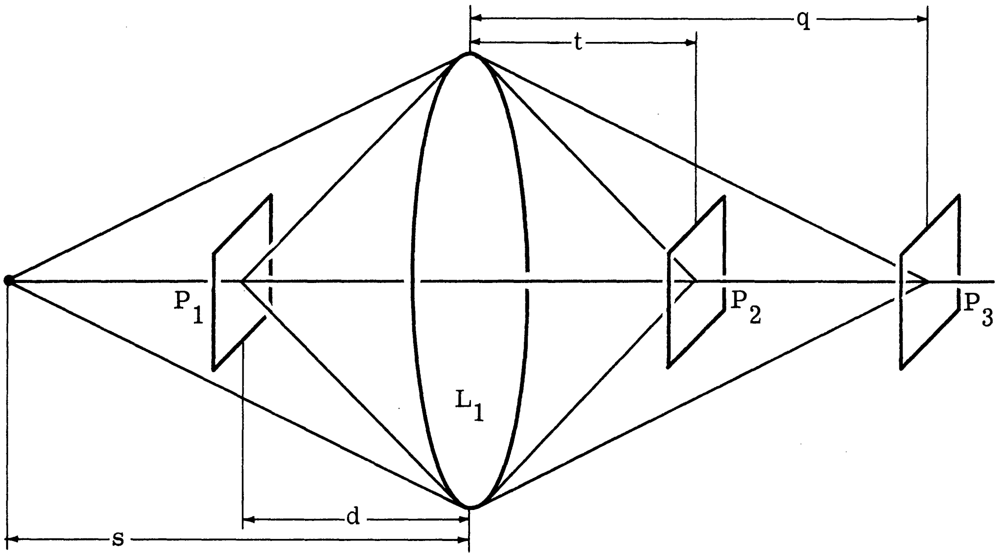

FIGURE 23. ONE-LENS SYSTEM

is not located in the back focal plane of the lens. We first find a relationship between the frequency variable p and a distance variable ξ in plane P_2. Referring to Diagram 3, we have

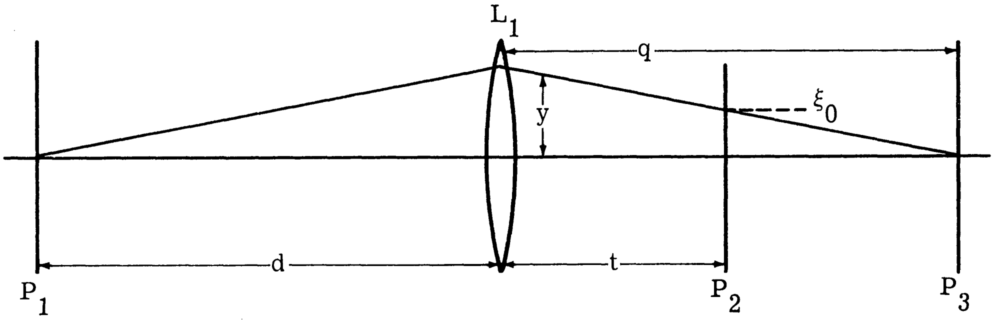

DIAGRAM 3

$$p = \frac{2\pi y}{\lambda d}$$

and

$$\frac{\xi}{q - t} = \frac{y}{t}$$

Therefore

$$p = \frac{2\pi t \xi}{\lambda d(q - t)}$$

To find the range on the signal aperture we refer to the sketch in Diagram 4. Since θ is small

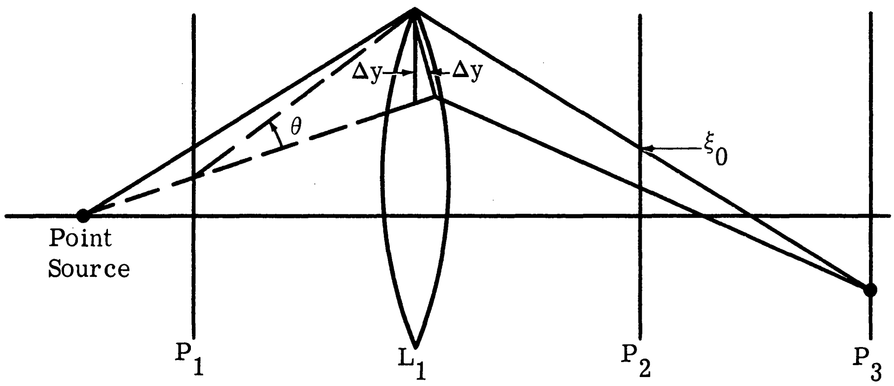

DIAGRAM 4

(d > f) we can make the approximation that $\Delta y \approx \Delta y_1$. Then, in terms of the maximum frequency in the signal, we have

$$\Delta y = \frac{t\lambda f p_o}{2\pi(q - t)}$$

and

$$y = \frac{s}{s - d} x$$

We require that $(y + \Delta y) < A$. Thus

$$\left[\frac{xs}{s - d} + \frac{t\lambda f p_o}{2\pi(q - t)}\right] < A$$

or, for space invariance,

$$|x| < \frac{s - d}{s}\left[A - \frac{p_o \lambda f t}{2\pi(q - t)}\right]$$

The total system length is s + q, and it is difficult to minimize this distance since the amount of signal aperture is also dependent on it. It is clear, however, that the maximum frequency response of this system is good. If one is willing to work with a small signal aperture, the system length can be kept reasonably short.

B.3.4. COMPARISON OF THE THREE SYSTEMS. It will simplify the comparison of these systems if we give numerical values to the system parameters. Suppose that

$$P_o/2\pi = 50\ l/mm$$
$$A = 25\ mm$$
$$\lambda = 5000\ \text{Å}$$
$$f = 200\ mm$$

To fix the parameters for the one-lens system, let

$$d = 2f = q$$
$$S = 4f$$
$$t = 4/3\ f$$

Substituting these parameters in the one-lens system formula gives

$$|X| < \frac{1}{2}\left(A - \frac{p_o \lambda f}{\pi}\right)$$

The systems are compared in the table.

The three-lens system is clearly superior on the basis of all three methods of comparison. The one- and two-lens systems have equal frequency response, but the signal aperture in the one-lens system is only half that of the two-lens system. This waste of system aperture should be avoided by using one of the other two systems; doing so reduces the length of the system also.

TABLE: COMPARISON OF THREE OPTICAL SYSTEMS

	One-Lens System	Two-Lens System	Three-Lens System
$\frac{p_{max}}{2\pi}$	125 l/m	125 l/m	250 l/m
Range on $\|X\|$ for $\frac{p_{max}}{2\pi} = 50$ l/m	7.5 mm or 30% of aperture	15 mm or 60% of aperture	20 mm or 80% of aperture
Total system length	1200 mm	1000 mm	600 mm

REFERENCES

1. T. P. Cheatham, Jr., and A. Kohlenberg, "Optical Filters—Their Equivalence to and Differences from Electrical Networks," IRE Intern Conv Record, 1954, Part 4, Electronic Computers and Information Theory, pp. 6-12.
2. E. O'Neill, "Spatial Filtering in Optics," IRE Trans Inform Theory, Vol. IT-2, No. 2, June 1956, pp. 56-65.
3. A. Maréchal, "Filtering of Optical Images," Communication and Information Theory Aspects of Modern Optics, General Electric Company, Electronics Laboratory, Syracuse, New York, August 1962.
4. D. Gabor, "Microscopy by Reconstructed Wave-Fronts," Part I, Proc. Roy. Soc. (London), Ser. A, 194, p. 454, 1949.
5. E. N. Leith, "Reconstructed Wavefronts and Communication Theory," J. Opt. Soc. Am., October 1962, Vol. 52, No. 10, pp. 1123-1130.
6. L. J. Cutrona, E. N. Leith, C. J. Palermo, and L. J. Porcello, "Optical Data Processing and Filtering Systems," IRE Trans Inform Theory, Vol. IT-6, No. 3, June 1960, p. 391.
7. M. Born and E. Wolf, Principles of Optics, Pergamon Press, New York, 1959, p. 359.

PROJECT MICHIGAN DISTRIBUTION LIST 4
1 July 1963 — Effective Date

Copy No.	Addressee
1	Office, Chief of Research & Development Department of the Army, Washington 25, D. C. ATTN: Chief, Communications-Electronics Division
2-3	Office, Deputy Chief of Staff for Military Operations Department of the Army, Washington 25, D. C. ATTN: Director, Organization and Training
4	Office, Assistant Chief of Staff for Intelligence Department of the Army, Washington 25, D. C. ATTN: Chief, Research & Development Branch
5	Commanding General, U. S. Army Electronics Command Fort Monmouth, New Jersey ATTN: AMSEL-RD
6-7	Commanding General, U. S. Army Electronics Command Fort Monmouth, New Jersey ATTN: AMSEL-CB
8-31	Commanding Officer, U. S. Army Electronics Research and Development Laboratory Fort Monmouth, New Jersey ATTN: SELRA/ADT
32	Commanding General, U. S. Army Electronic Proving Ground Fort Huachuca, Arizona ATTN: Technical Library
33	Office of the Director, Defense Research & Engineering Technical Library, Department of Defense Washington 25, D. C.
34	Director, Weapons Systems Evaluation Group Room 1E875, The Pentagon Washington 25, D. C.
35	Commanding General, U. S. Army Materiel Command Department of the Army, Washington 25, D. C. ATTN: AMCRD-DE-MO
36	Chief of Ordnance, Research & Development Division Department of the Army, Washington 25, D. C. ATTN: ORDTB, Research & Special Projects
37	Army Research and Engineering Center Kansas Street Natick, Massachusetts ATTN: Technical Library
38	Chief, Human Factors Research Division Office of the Chief of Research & Development Department of the Army, Washington 25, D. C.
39-43	Chief, U. S. Army Security Agency Arlington Hall Station Arlington 12, Virginia
(39)	ATTN: Technical Consultant
(40)	ATTN: ACofS, Developments
(41)	ATTN: Deputy President USASA Board
(42-43)	ATTN: ACofS, G3
44	Commanding Officer U. S. Army Air Defense CD Agency Fort Bliss 16, Texas
45-46	Commanding General, U. S. Army Ordnance Missile Command Redstone Arsenal, Alabama ATTN: Technical Library
47-48	Commanding General Army Tank-Automotive Command 1501 Beard Street Detroit 9, Michigan ATTN: ORDMC-RF
49	Commanding General Army Medical Research & Development Command Main Navy Building Washington 25, D. C. ATTN: Neuropsychiatry & Psychophysiology Research Branch
50-51	U. S. Army Personnel Research Office Washington 25, D. C. ATTN: CRD-AI
52	Commanding Officer U. S. Army Diamond Ordnance Fuze Laboratories Washington 25, D. C. ATTN: AMXDO-TI
53-56	Director, U. S. Army Engineer Geodesy Intelligence & Mapping Research & Development Agency Fort Belvoir, Virginia
(53)	ATTN: Intelligence Division
(54)	ATTN: Research & Analysis Division
(55)	ATTN: Photogrammetry Division
(56)	ATTN: Strategic Systems Division (ENGGM-SS)
57	Director, U. S. Army Cold Regions Research & Engineering Laboratory P. O. Box 282 Hanover, New Hampshire
58-60	Director, U. S. Army Engineers Research & Development Laboratory Fort Belvoir, Virginia
(58)	ATTN: Chief, Electrical Department
(59-60)	ATTN: Technical Documents Center
61	Commanding Officer U. S. Army Research Office (Durham) Box CM, Duke Station Durham, North Carolina ATTN: Chief Information Processing Office
62	Commanding General, U. S. Army Combat Development Experimentation Center, Fort Ord, California ATTN: File CDEC-CG
63	Director, Human Engineering Laboratory Aberdeen Proving Ground, Aberdeen, Maryland
64	Commandant, U. S. Army Command & General Staff College, Fort Leavenworth, Kansas ATTN: Archives
65	Commanding Officer, Infantry Combat Developments Agency Fort Benning, Georgia
66	Commanding Officer, U. S. Army Armor Combat Development Field Agency Fort Knox, Kentucky
67	Commanding Officer, U. S. Army Artillery Combat Development Agency Fort Sill, Oklahoma ATTN: TA Branch
68	Assistant Commandant, U. S. Army Air Defense School Fort Bliss, Texas

PROJECT MICHIGAN DISTRIBUTION LIST 4 (Continued)

Copy No.	Addressee
69	Commandant, U. S. Army Engineer School Fort Belvoir, Virginia ATTN: ESSY-L
70	Director, Engineer Combat Developments Agency Building NN-19 Fort Belvoir, Virginia
71	President, U. S. Army Infantry Board Fort Benning, Georgia
72	President, U. S. Army Artillery Board Fort Sill, Oklahoma
73	President, U. S. Army Air Defense Board Fort Bliss, Texas
74	President, U. S. Army Aviation Board Fort Rucker, Alabama
75	President, U. S. Army Airborne Electronics and Special Warfare Board, Fort Bragg, North Carolina
76	Commanding Officer, U. S. Army Intelligence Materiel Development Agency Fort Holabird, Baltimore 19, Maryland
77	Commanding Officer, U. S. Army Intelligence Combat Development Agency Fort Holabird, Baltimore 19, Maryland
78-80	U. S. Army Research Liaison Office, MIT-Lincoln Laboratory Lexington 73, Massachusetts
81-82	Office, Deputy Chief of Naval Operations Department of the Navy The Pentagon Washington 25, D. C. ATTN: Op-07T
83	Office of Naval Research, Department of the Navy 17th & Constitution Avenue, N. W. Washington 25, D. C. ATTN: Code 461
84	The Hydrographer, U. S. Navy Hydrographic Office Washington 25, D. C. ATTN: Code 1640
85-90	Chief, Bureau of Ships, Department of the Navy Washington 25, D. C.
(85)	ATTN: Code 335
(86)	ATTN: Code 607A
(87)	ATTN: Code 687C
(88-90)	ATTN: Code 362A
91	Bureau of Naval Weapons, Department of the Navy Washington 25, D. C. ATTN: RTOS-3
92-93	Director, U. S. Naval Research Laboratory Washington 25, D. C. ATTN: Code 2027
94	Commanding Officer, U. S. Navy Ordnance Laboratory Corona, California ATTN: Library
95	Commanding Officer & Director U. S. Navy Electronics Laboratory San Diego 52, California ATTN: Library
96	U. S. Naval Missile Center Point Mugu, California ATTN: Code N223, Space Research Division Astronautics Department
97	Commanding Officer U. S. Naval Ordnance Test Station China Lake, California ATTN: Analysis Branch, Code 3515
98	Avionics Branch, Nucleonics Division Directorate of Research, DCS/R&T HQ USAF, The Pentagon Washington 25, D. C.
99	Commander in Chief, Headquarters, Strategic Air Command Offutt Air Force Base, Nebraska ATTN: DICC
100	Headquarters, USAF, Directorate of Operation Requirements Washington 25, D. C. ATTN: AFORQ
101	Air Force Intelligence Center Arlington Hall Station Arlington 12, Virginia ATTN: AFCIN-3H2
102-105	Headquarters Tactical Air Command Langley AFB, Virginia
(102)	ATTN: DORQ (Requirements)
(103)	ATTN: DOC (Communications-Electronics)
(104-105)	ATTN: OA (Operations Analysis)
106	Foreign Technology Division Wright-Patterson AFB, Ohio ATTN: TD-Blb(2)
107-131	ASTIA (TIPCA) Arlington Hall Station Arlington 12, Virginia
132	Headquarters, 6570th Aerospace Medical Research Laboratories (MRVPV) Wright-Patterson AFB, Ohio
133-136	Commander Wright-Patterson AFB, Ohio
(133)	ATTN: ASD (ASRNOO)
(134)	ATTN: ASD (ASAPR-D)
(135-136)	ATTN: ASD (ASRNGE-1)
137-140	Commander, Rome Air Development Center Griffiss AFB, New York
(137)	ATTN: RAALD
(138)	ATTN: RADC (RASH)
(139)	ATTN: RAWIC
(140)	ATTN: RALSS
141-142	Commander, AFESD Laurence G. Hanscom Field Bedford, Massachusetts ATTN: ESRHA-Stop 36
143	APGC (PGAPI) Eglin Air Force Base, Florida
144	Commandant of the Marine Corps Headquarters, U. S. Marine Corps Washington 25, D. C. ATTN: Code AO2

PROJECT MICHIGAN DISTRIBUTION LIST 4 (Continued)

Copy No.	Addressee
145	Director, Marine Corps Landing Force Development Center, Marine Corps Schools Quantico, Virginia
146-150	Central Intelligence Agency 2430 E Street, N. W. Washington 25, D. C. ATTN: OCR Mail Room
151-152	Scientific & Technical Information Facility P. O. Box 5700 Bethesda, Maryland ATTN: NASA Representative
153-154	National Aeronautics & Space Administration Manned Space Craft Center Houston 1, Texas ATTN: Chief, Technical Information Division
155	Cornell Aeronautical Laboratory, Incorporated Washington Projects Office 1114 Leesburg Pike Falls Church, Virginia ATTN: Technical Library
156	The Rand Corporation 1700 Main Street Santa Monica, California ATTN: Library
157	Research Analysis Corporation 6935 Arlington Road Bethesda, Maryland Washington 14, D. C. ATTN: Chief, Information and Control Systems Division
158-159	Cornell Aeronautical Laboratory, Incorporated 4455 Genesee Street Buffalo 21, New York ATTN: Librarian VIA: Bureau of Naval Weapons, Representative 4455 Genesee Street Buffalo 21, New York
160-161	Director, Human Resources Research Office The George Washington University 300 North Washington Street Alexandria, Virginia ATTN: Library
162	Chief, U. S. Army Aviation HRU P. O. Box 428 Fort Rucker, Alabama
163	Chief, U. S. Army Air Defense Research Unit Fort Bliss, Texas
164	Chief, U. S. Army Armor Human Research Unit Fort Knox, Kentucky
165	U. S. Naval Photographic Interpretation Center 4301 Suitland Road Washington 25, D. C.
166	Coordinated Science Laboratory University of Illinois Urbana, Illinois ATTN: Librarian VIA: ONR Resident Representative 605 S. Goodwin Avenue Urbana, Illinois
167	Visibility Laboratory, Scripps Institution of Oceanography University of California San Diego 52, California
168	The Ohio State University, Research Foundation 1314 Kinnear Road Columbus 12, Ohio ATTN: Security Office VIA: Commander, Wright Air Development Division Wright-Patterson AFB, Ohio ATTN: ASRKSE
169-171	Jet Propulsion Laboratory California Institute of Technology 4800 Oak Grove Drive Pasadena, California
172-173	Commanding Officer, Pictinny Arsenal Dover, New Jersey ATTN: SMUPA-DW9
174	Commanding Officer, U. S. Army Liaison Group, Project MICHIGAN The University of Michigan P. O. Box 618 Ann Arbor, Michigan

AD Div. 6/6

Inst. of Science and Technology, U. of Mich., Ann Arbor SIGNAL DETECTION BY COMPLEX SPATIAL FILTERING, by A. B. VanderLugt. Report of Project MICHIGAN. July 63. 39 p. incl. illus., table, 7 refs.
(Report No. 2900-394-T/4594-22-T)
(Contracts DA-36-039 SC-78801 and AF 33(616)-8433)
Unclassified report

This report contains integrated descriptions of the problem of signal detection, the optimum linear filtering process, a coherent optical system which accomplishes this filtering process, and a technique for realizing the required complex filter. Experimental results show that the theory is valid. The appendixes give a treatment of the Fourier transforming property of lenses which is general enough that complete optical systems can be evaluated on the basis of frequency response and region of space-invariant operation.
(over)

UNCLASSIFIED

I. Title: Project MICHIGAN
II. VanderLugt, A. B.
III. U. S. Army Electronics Command
IV. U. S. Air Force
V. Contract DA-36-039 SC-78801
VI. Contract AF 33(616)-8433

UNCLASSIFIED

AD Div. 6/6

Inst. of Science and Technology, U. of Mich., Ann Arbor SIGNAL DETECTION BY COMPLEX SPATIAL FILTERING, by A. B. VanderLugt. Report of Project MICHIGAN. July 63. 39 p. incl. illus., table, 7 refs.
(Report No. 2900-394-T/4594-22-T)
(Contracts DA-36-039 SC-78801 and AF 33(616)-8433)
Unclassified report

This report contains integrated descriptions of the problem of signal detection, the optimum linear filtering process, a coherent optical system which accomplishes this filtering process, and a technique for realizing the required complex filter. Experimental results show that the theory is valid. The appendixes give a treatment of the Fourier transforming property of lenses which is general enough that complete optical systems can be evaluated on the basis of frequency response and region of space-invariant operation.
(over)

UNCLASSIFIED

I. Title: Project MICHIGAN
II. VanderLugt, A. B.
III. U. S. Army Electronics Command
IV. U. S. Air Force
V. Contract DA-36-039 SC-78801
VI. Contract AF 33(616)-8433

UNCLASSIFIED

AD Div. 6/6

Inst. of Science and Technology, U. of Mich., Ann Arbor SIGNAL DETECTION BY COMPLEX SPATIAL FILTERING, by A. B. VanderLugt. Report of Project MICHIGAN. July 63. 39 p. incl. illus., table, 7 refs.
(Report No. 2900-394-T/4594-22-T)
(Contracts DA-36-039 SC-78801 and AF 33(616)-8433)
Unclassified report

This report contains integrated descriptions of the problem of signal detection, the optimum linear filtering process, a coherent optical system which accomplishes this filtering process, and a technique for realizing the required complex filter. Experimental results show that the theory is valid. The appendixes give a treatment of the Fourier transforming property of lenses which is general enough that complete optical systems can be evaluated on the basis of frequency response and region of space-invariant operation.
(over)

UNCLASSIFIED

I. Title: Project MICHIGAN
II. VanderLugt, A. B.
III. U. S. Army Electronics Command
IV. U. S. Air Force
V. Contract DA-36-039 SC-78801
VI. Contract AF 33(616)-8433

UNCLASSIFIED

AD Div. 6/6

Inst. of Science and Technology, U. of Mich., Ann Arbor SIGNAL DETECTION BY COMPLEX SPATIAL FILTERING, by A. B. VanderLugt. Report of Project MICHIGAN. July 63. 39 p. incl. illus., table, 7 refs.
(Report No. 2900-394-T/4594-22-T)
(Contracts DA-36-039 SC-78801 and AF 33(616)-8433)
Unclassified report

This report contains integrated descriptions of the problem of signal detection, the optimum linear filtering process, a coherent optical system which accomplishes this filtering process, and a technique for realizing the required complex filter. Experimental results show that the theory is valid. The appendixes give a treatment of the Fourier transforming property of lenses which is general enough that complete optical systems can be evaluated on the basis of frequency response and region of space-invariant operation.
(over)

UNCLASSIFIED

I. Title: Project MICHIGAN
II. VanderLugt, A. B.
III. U. S. Army Electronics Command
IV. U. S. Air Force
V. Contract DA-36-039 SC-78801
VI. Contract AF 33(616)-8433

UNCLASSIFIED

AD

The experimental results obtained to data indicate that this technique provides an excellent two-dimensional filtering capability that will play a key role in problems such as shape recognition and signal detection.

UNCLASSIFIED

DESCRIPTORS

Optical filters
Lenses
Interferometers
Optical equipment

UNCLASSIFIED

AD

The experimental results obtained to data indicate that this technique provides an excellent two-dimensional filtering capability that will play a key role in problems such as shape recognition and signal detection.

UNCLASSIFIED

DESCRIPTORS

Optical filters
Lenses
Interferometers
Optical equipment

UNCLASSIFIED

AD

The experimental results obtained to data indicate that this technique provides an excellent two-dimensional filtering capability that will play a key role in problems such as shape recognition and signal detection.

UNCLASSIFIED

DESCRIPTORS

Optical filters
Lenses
Interferometers
Optical equipment

UNCLASSIFIED

AD

The experimental results obtained to data indicate that this technique provides an excellent two-dimensional filtering capability that will play a key role in problems such as shape recognition and signal detection.

UNCLASSIFIED

DESCRIPTORS

Optical filters
Lenses
Interferometers
Optical equipment

UNCLASSIFIED

AD Div. 6/6

Inst. of Science and Technology, U. of Mich., Ann Arbor
SIGNAL DETECTION BY COMPLEX SPATIAL FILTERING, by A. B. VanderLugt. Report of Project MICHIGAN. July 63. 39 p. incl. illus., table, 7 refs.
(Report No. 2900-394-T/4594-22-T)
(Contracts DA-36-039 SC-78801 and AF 33(616)-8433)
Unclassified report

This report contains integrated descriptions of the problem of signal detection, the optimum linear filtering process, a coherent optical system which accomplishes this filtering process, and a technique for realizing the required complex filter. Experimental results show that the theory is valid. The appendixes give a treatment of the Fourier transforming property of lenses which is general enough that complete optical systems can be evaluated on the basis of frequency response and region of space-invariant operation.

(over)

UNCLASSIFIED

I. Title: Project MICHIGAN
II. VanderLugt, A. B.
III. U. S. Army Electronics Command
IV. U. S. Air Force
V. Contract DA-36-039 SC-78801
VI. Contract AF 33(616)-8433

UNCLASSIFIED

AD Div. 6/6

Inst. of Science and Technology, U. of Mich., Ann Arbor
SIGNAL DETECTION BY COMPLEX SPATIAL FILTERING, by A. B. VanderLugt. Report of Project MICHIGAN. July 63. 39 p. incl. illus., table, 7 refs.
(Report No. 2900-394-T/4594-22-T)
(Contracts DA-36-039 SC-78801 and AF 33(616)-8433)
Unclassified report

This report contains integrated descriptions of the problem of signal detection, the optimum linear filtering process, a coherent optical system which accomplishes this filtering process, and a technique for realizing the required complex filter. Experimental results show that the theory is valid. The appendixes give a treatment of the Fourier transforming property of lenses which is general enough that complete optical systems can be evaluated on the basis of frequency response and region of space-invariant operation.

(over)

UNCLASSIFIED

I. Title: Project MICHIGAN
II. VanderLugt, A. B.
III. U. S. Army Electronics Command
IV. U. S. Air Force
V. Contract DA-36-039 SC-78801
VI. Contract AF 33(616)-8433

UNCLASSIFIED

AD Div. 6/6

Inst. of Science and Technology, U. of Mich., Ann Arbor
SIGNAL DETECTION BY COMPLEX SPATIAL FILTERING, by A. B. VanderLugt. Report of Project MICHIGAN. July 63. 39 p. incl. illus., table, 7 refs.
(Report No. 2900-394-T/4594-22-T)
(Contracts DA-36-039 SC-78801 and AF 33(616)-8433)
Unclassified report

This report contains integrated descriptions of the problem of signal detection, the optimum linear filtering process, a coherent optical system which accomplishes this filtering process, and a technique for realizing the required complex filter. Experimental results show that the theory is valid. The appendixes give a treatment of the Fourier transforming property of lenses which is general enough that complete optical systems can be evaluated on the basis of frequency response and region of space-invariant operation.

(over)

UNCLASSIFIED

I. Title: Project MICHIGAN
II. VanderLugt, A. B.
III. U. S. Army Electronics Command
IV. U. S. Air Force
V. Contract DA-36-039 SC-78801
VI. Contract AF 33(616)-8433

UNCLASSIFIED

AD Div. 6/6

Inst. of Science and Technology, U. of Mich., Ann Arbor
SIGNAL DETECTION BY COMPLEX SPATIAL FILTERING, by A. B. VanderLugt. Report of Project MICHIGAN. July 63. 39 p. incl. illus., table, 7 refs.
(Report No. 2900-394-T/4594-22-T)
(Contracts DA-36-039 SC-78801 and AF 33(616)-8433)
Unclassified report

This report contains integrated descriptions of the problem of signal detection, the optimum linear filtering process, a coherent optical system which accomplishes this filtering process, and a technique for realizing the required complex filter. Experimental results show that the theory is valid. The appendixes give a treatment of the Fourier transforming property of lenses which is general enough that complete optical systems can be evaluated on the basis of frequency response and region of space-invariant operation.

(over)

UNCLASSIFIED

I. Title: Project MICHIGAN
II. VanderLugt, A. B.
III. U. S. Army Electronics Command
IV. U. S. Air Force
V. Contract DA-36-039 SC-78801
VI. Contract AF 33(616)-8433

UNCLASSIFIED

AD

The experimental results obtained to data indicate that this technique provides an excellent two-dimensional filtering capability that will play a key role in problems such as shape recognition and signal detection.

UNCLASSIFIED

DESCRIPTORS

Optical filters
Lenses
Interferometers
Optical equipment

UNCLASSIFIED

AD

The experimental results obtained to data indicate that this technique provides an excellent two-dimensional filtering capability that will play a key role in problems such as shape recognition and signal detection.

UNCLASSIFIED

DESCRIPTORS

Optical filters
Lenses
Interferometers
Optical equipment

UNCLASSIFIED

AD

The experimental results obtained to data indicate that this technique provides an excellent two-dimensional filtering capability that will play a key role in problems such as shape recognition and signal detection.

UNCLASSIFIED

DESCRIPTORS

Optical filters
Lenses
Interferometers
Optical equipment

UNCLASSIFIED

AD

The experimental results obtained to data indicate that this technique provides an excellent two-dimensional filtering capability that will play a key role in problems such as shape recognition and signal detection.

UNCLASSIFIED

DESCRIPTORS

Optical filters
Lenses
Interferometers
Optical equipment

UNCLASSIFIED

July 1963

Report of Project MICHIGAN
2900-394-T

SIGNAL DETECTION BY COMPLEX SPATIAL FILTERING

A. B. Vander Lugt

ERRATA

Page	Line	Change
6	Fig. 3	For f between P_1 and L_1 read d
38	Table	For m read mm (4 occurrences)